CHAPTER THIRTEEN

Methylphosphonic Acid Biosynthesis and Catabolism in Pelagic Archaea and Bacteria

Emily C. Ulrich*, Siddhesh S. Kamat[†,1], Bjarne Hove-Jensen[‡,1], David L. Zechel[§,1]

*Carl R. Woese Institute for Genomic Biology, University of Illinois at Urbana—Champaign, Urbana, IL, United States
[†]Indian Institute of Science Education and Research (IISER), Pune, Maharashtra, India
[‡]Aarhus University, Aarhus, Denmark
[§]Queen's University, Kingston, ON, Canada
[1]Corresponding authors: e-mail address: siddhesh@iiserpune.ac.in; hove@mbg.au.dk; dlzechel@chem.queensu.ca

Contents

Methods in Enzymology, Volume 605
ISSN 0076-6879
https://doi.org/10.1016/bs.mie.2018.01.039

Abstract

Inorganic phosphate is essential for all life forms, yet microbes in marine environments are in near constant deprivation of this important nutrient. Organophosphonic acids can serve as an alternative source of inorganic phosphate if microbes possess the appropriate biochemical pathways that allow cleavage of the stable carbon–phosphorus bond that defines this class of molecule. One prominent source of inorganic phosphate is methylphosphonic acid, which is found as a constituent of marine-dissolved organic matter. The cycle of biosynthesis and catabolism of methylphosphonic acid by marine microbes is the likely source of supersaturating levels of methane in shallow ocean waters. This review provides an overview of the rich biochemistry that has evolved to synthesize methylphosphonic acid and catabolize this molecule into Pi and methane, with an emphasis on the reactions catalyzed by methylphosphonic acid synthase MpnS and the carbon–phosphorus lyase system. The protocols and experiments that are described for MpnS and carbon–phosphorus lyase provide a foundation for studying the structures and mechanisms of these and related enzymes.

1. INTRODUCTION

1.1 The Methane Paradox

Methane is a potent greenhouse gas with numerous anthropogenic, biotic, and abiotic sources. It is also consumed globally though combustion and microbial oxidation. Because methane plays such a prominent role in atmospheric chemistry, it is necessary to estimate the net flux of this molecule by accounting for sources and sinks in a global methane budget. Current estimates place the world's oceans and freshwater lakes as a minor contributor to global methane emissions, estimated to be 2% of the global total of 0.5 megatones per year (reviewed in depth by Reeburgh) (Reeburgh, 2007). The distribution of methane in the oceanic water columns has long presented a scientific mystery. The ocean can be viewed primarily as a vessel for microbial oxidation of methane, which results in low nanomolar concentrations throughout the water column that are either at equilibrium or undersaturated with respect to the atmosphere. The exception is a spike in methane concentration to 5 n*M* at a depth (100–150 m) that lies just above the thermocline that separates warmer surface-mixed waters from deeper and colder waters (Fig. 1; Scranton & Brewer, 1977). This spike, referred to as the mixed methane layer maximum, has perplexed scientists since the 1970s, as 5 n*M* methane is supersaturating with respect to the atmosphere, and thus implies net generation of methane in shallow ocean waters. While methanogenesis by anaerobic bacteria is well known, this pathway

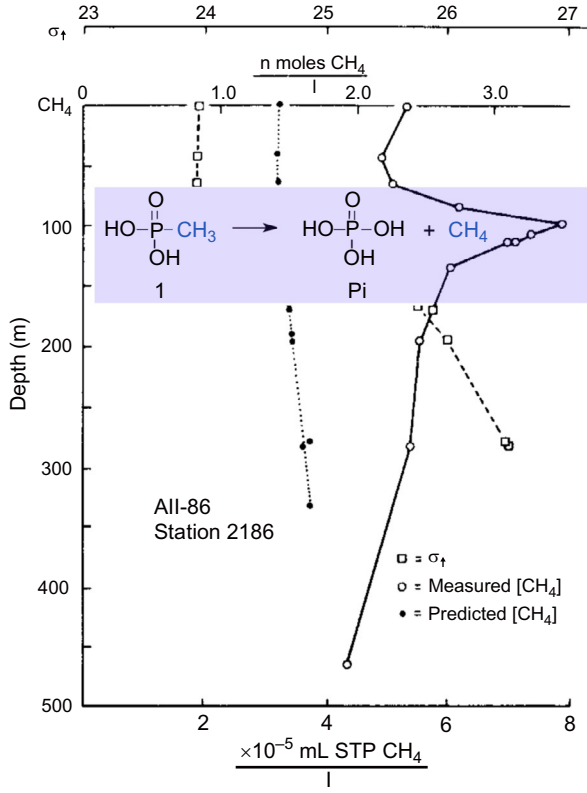

Fig. 1 Variation in methane concentration (*open circles*) with ocean depth at a station approximately 500 km East of Puerto Rico (Scranton & Brewer, 1977). *Figure adapted with permission from Elsevier.*

requires anoxic conditions that are only available in the sediments of the ocean floor. The paradox presented by saturating levels of methane in shallow, oxygen-rich ocean waters has spurred a decade's long hunt for a less oxygen-sensitive pathway for methane production. Only recently does evidence suggest that the "ocean methane paradox" is the product of microorganisms living in the mixed surface waters, which degrade methylphosphonic acid **1** into methane and inorganic phosphate (Pi) (Karl et al., 2008; Repeta et al., 2016).

The formation of methane from **1** arises from an elaborate enzymatic reaction that has evolved to produce Pi from alkylphosphonic acids (Pn) by cleaving a chemically inert carbon–phosphorus (C—P) bond. While Pi is a central ion that underpins the biochemistry of all life forms, a shadow phosphorus biochemistry has evolved in microorganisms that is based on the

biosynthesis and catabolism of Pn, of which **1** is the simplest example. While Pn are better known to the public as synthetic compounds, with the herbicide glyphosate (RoundUp) being the best example, a large number of Pn also occur as natural products, serving structural and antibiotic roles for the organisms that produce them. Some well-known examples include 2-aminoethylphosphonic acid **2**, the most common naturally occurring Pn, fosfomycin **3**, a widely used antibiotic, and the herbicide phosphinothricin **4** (Fig. 2). Within the Pn natural product family **1** is part of a small subset of structurally simple Pn that are known to either serve as building blocks to create more complex natural products, or to serve as sources of Pi when this nutrient is limiting (reviewed in Horsman & Zechel, 2017). Some of these, notably **1** (Metcalf et al., 2012; Sosa et al., 2017), **2**, 2-amino-1-hydroxyethylphosphonic acid (Watanabe et al., 2001), and 2-hydroxyethylphosphonic acid **8** (Kaya et al., 2006; Sosa et al., 2017; Yu, Price, Evans, & Metcalf, 2014), are observed to appear as Pn esters with lipids, polysaccharides, and proteins. Incorporation of Pn into other biomolecules can occur to surprisingly high levels: up to 60% of the phospholipids in the cilia of the rumen protozoan *Tetrahymena pyriformis* have **2** in place of phosphocholine as a head group (Kennedy & Thompson, 1970). Such biomolecules comprise the dissolved organic matter of marine environments that sustains microbial growth. Recently, ^{31}P NMR spectroscopy was used to directly observe **1**, **8**, and hydroxymethylphosphonic acid **17** as the most abundant Pn associated with the polysaccharide fraction of dissolved organic matter that was isolated from the ALOHA station near Hawaii (Repeta et al., 2016). Similarly, ^{31}P NMR spectroscopy has shown that the cyanobacterium *Trichodesmium erythraeum* IMS101 can synthesize Pn, most likely **1** and **2**, and incorporate these compounds into lipids, proteins, and glycans such that 10% of the total biomolecule-associated phosphorus is represented by Pn (Dyhrman, Benitez-Nelson, Orchard, Haley, & Pellechia, 2009). This strategy appears to be widespread in cyanobacteria, which have been shown to use Pn such as **2**, a near perfect surrogate for phosphoethanolamine, as head groups for lipids under Pi limiting conditions (Van Mooy et al., 2009). This suggests

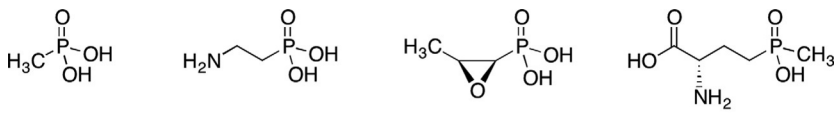

1 **2** **3** **4**

Fig. 2 Examples of Pn natural products. Methylphosphonic acid **1**, 2-aminoethylphosphonic acid **2**, fosfomycin **3**, and phosphinothricin **4**.

that in addition to serving as a Pi source and a motif for antibiotic biosynthesis, Pn can serve a third role in *reducing* the demand for Pi in biosynthesis. It has been estimated that using Pn to synthesize phosphonolipids can reduce the total cellular phosphorus demand by 10–40% (Van Mooy et al., 2009). Therefore, in marine microbes, we find an intriguing biochemical cycle of Pn synthesis, storage, and catabolism, sometimes all within a single species.

1.2 Biosynthesis of Methylphosphonic Acid

The simple structure of **1** belies a rich biochemistry, largely shared with other Pn natural products, that is dedicated to its biosynthesis and catabolism. The biosynthesis of **1**, like almost all known Pn natural products, begins with the formation of the C—P bond (Scheme 1). This occurs through the reversible conversion of phosphoenolpyruvate **5** to phosphonopyruvate **6** by the enzyme phosphoenolpyruvate mutase (PepM) (Seidel, Freeman, Seto, & Knowles, 1988). Because this reaction is common to almost all of the discovered natural product Pn, the gene encoding PepM can be used as a marker to identify Pn biosynthetic gene clusters in genomes, and even phylogenetically predict Pn structural diversity (Ju et al., 2015; Ju, Doroghazi, & Metcalf, 2014; Yu et al., 2013). The equilibrium between **5** and **6** is unfavorable due to the greater strength of the O—P bond relative to the C—P bond (Bowman, McQueney, Barry, & Dunaway-Mariano, 1988); therefore the next reaction is irreversible, involving the decarboxylation of **6** by the thiamine pyrophosphate-dependent enzyme phosphonopyruvate decarboxylase (Ppd). The product, phosphonoacetaldehyde **7**, is reduced by a NAD^+/NADH-dependent dehydrogenase (Pdh) to form 2-hydroxyethylphosphonic acid **8**, a key intermediate in the biosynthesis of a number of Pn (Shao et al., 2008), and the penultimate precursor to **1**.

1.2.1 Methylphosphonic Acid Synthase

The C—C bond cleaving step that converts **8** to **1** is a fascinating example of how evolution can repurpose the reactivity of a common enzyme scaffold. The enzyme catalyzing this step, methylphosphonic acid synthase (MpnS), was discovered by scanning the genome of *Nitrosopumilus maritimus*, a common marine archaeon, for Pn biosynthetic gene clusters using *pepM* as a probe (Metcalf et al., 2012). The gene encoding MpnS was found in association with three genes (*pepM*, *ppd*, *pdh*) necessary to encode the synthesis of **8**. MpnS belongs to a cupin subfamily of mononuclear nonheme Fe(II)-dependent enzymes that include hydroxypropylphosphonic acid epoxidase (HppE) (Kuzuyama, Seki, Kobayashi, Hidaka, & Seto, 1999; Liu et al.,

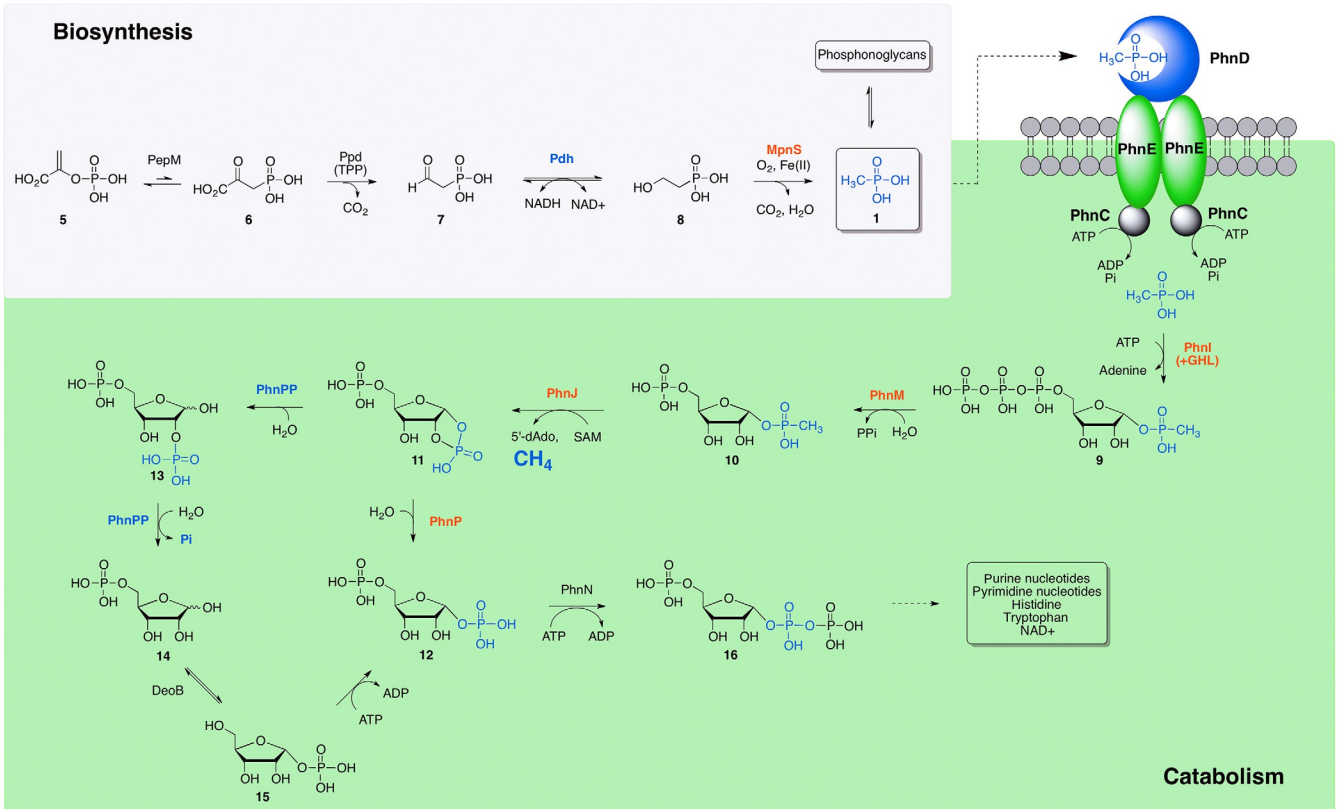

Scheme 1 Overview of the microbial biosynthesis of methylphosphonic acid **1** followed by its catabolism into phosphate containing metabolites and methane by the carbon–phosphorus lyase pathway.

2001) and 2-hydroxyethylphosphonate (**8**) dioxygenase (HEPD) (Cicchillo et al., 2009), which are involved in the biosynthesis of **3** and **4,** respectively. Unlike the better-known α-ketoglutarate-dependent family of nonheme Fe (II)-dependent dioxygenases, MpnS and HEPD function as oxygenases without a requirement for α-ketoglutarate as a cosubstrate (Scheme 2A and B). Both MpnS and HEPD cleave the C—C bond of **8**, but the fate of molecular oxygen differs in each enzyme.

The *N. maritimus* MpnS reaction is novel in that the C—C bond of **8** is cleaved to form **1** and CO_2 using only molecular oxygen and Fe(II). As the input of external electrons is not required for C—C bond cleavage, all four electrons that are used to reduce O_2 to H_2O are derived from **8**. A detailed mechanism for this unusual reaction has been proposed based on extensive studies with substrate analogs, isotopic labeling, site-directed mutagenesis, and X-ray crystallography (Born et al., 2017; Cooke, Peck, Evans, & van der Donk, 2012; Metcalf et al., 2012; Peck, Chekan, Ulrich, Nair, & van der Donk, 2015; Peck et al., 2017; Zhu, Peck, Bonnot, van der Donk, & Klinman, 2015). The X-ray crystal structure of *N. maritimus* MpnS revealed that the Fe(II) ion is coordinated by two histidine residues and one glutamine (Scheme 3A, **I**) (Born et al., 2017). Such Fe(II) coordination had

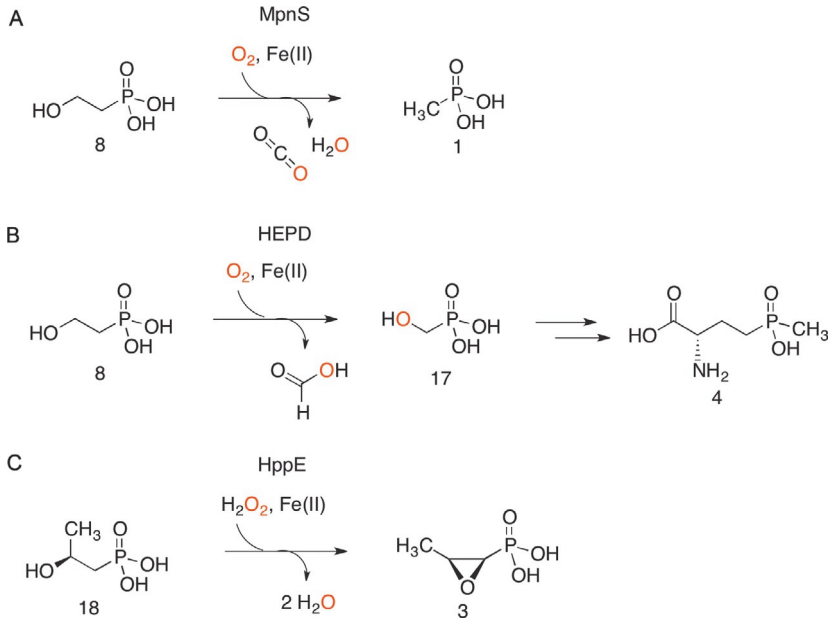

Scheme 2 Oxidative reactions catalyzed by methylphosphonic acid synthase (MpnS) (A) and the homologous Fe(II)-dependent enzymes 2-hydroxylethylphosphonic acid dioxygenase (HEPD) (B), and 2-hydroxypropylphosphonic acid epoxidase (HppE) (C).

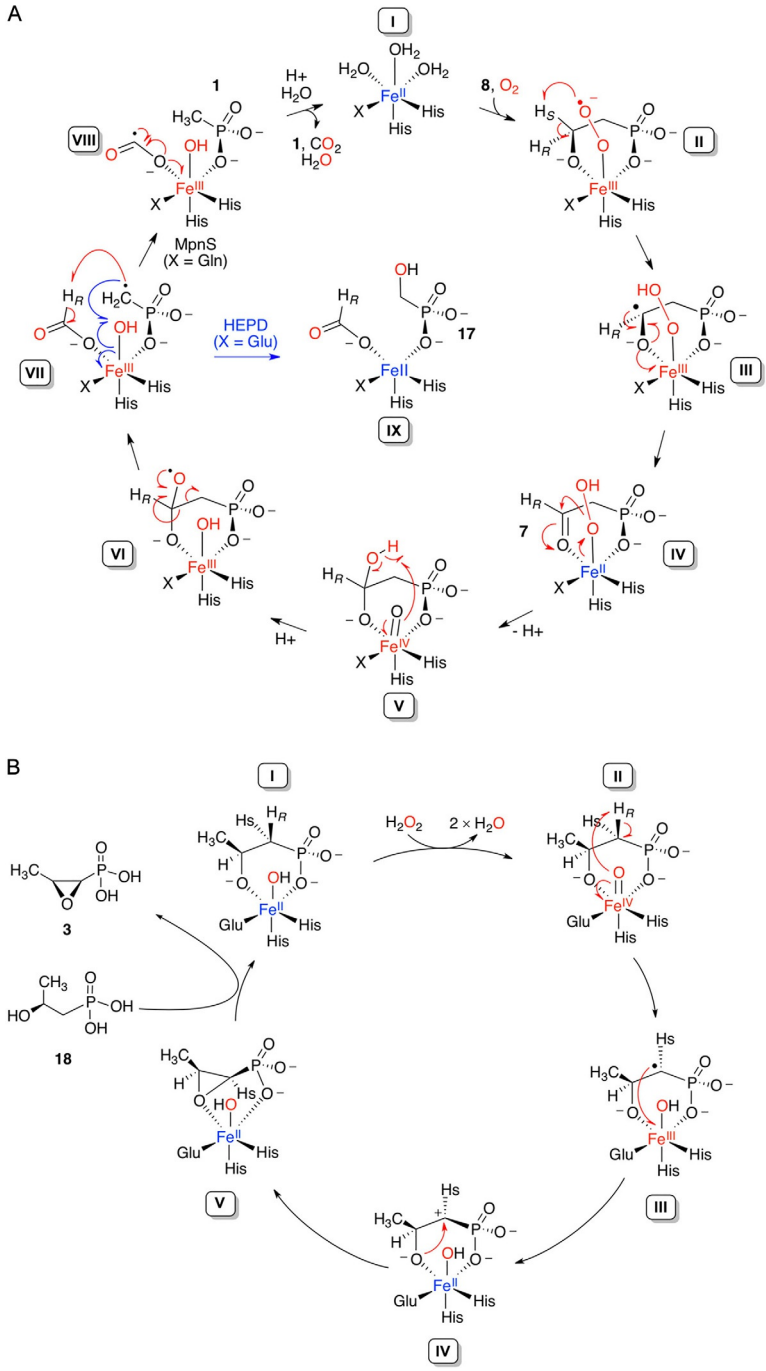

Scheme 3 Proposed mechanisms for (A) MpnS and HEPD contrasted with (B) HppE.

not been observed previously: mononuclear nonheme Fe(II) enzymes, including HEPD (Cicchillo et al., 2009) and HppE (Higgins, Yan, Liu, Liu, & Drennan, 2005), typically bind Fe(II) with two histidine residues and either an aspartate or a glutamate residue, called a 2-histidine/1-carboxylate facial triad. The substrate **8** is observed to bind to the Fe(II) nucleus in a bidentate fashion using a phosphoryl oxygen and the 2-hydroxyl (Born et al., 2017). Molecular oxygen is proposed to bind the Fe(II) center and be reduced to superoxide (Scheme 3A, **I** to **II**) (Cooke et al., 2012). Abstraction of the pro-*S* hydrogen of C2 forms a ketyl radical (**II** to **III**), which in turn reduces the Fe(III) ion to Fe(II) and forms phosphonoacetaldehyde **7** (**III** to **IV**). Attack of the bound hydroperoxide on the aldehyde with concomitant formation of a ferryl species is proposed (**IV** to **V**), which could also arise directly from homolytic scission of the peroxide bond to hydroxylate the ketyl radical (**III** directly to **V**) (Peck et al., 2017). The Fe(IV) oxo species then abstracts the hydroxyl hydrogen to form an alkoxy radical (**V** to **VI**), thereby promoting β-scission of the C—C bond (a common reaction for alkoxy radicals), and forming a methylphosphonate radical and formate (**VI** to **VII**). Hydrogen atom transfer from formate to the methylphosphonate radical forms **1**, while reduction of Fe(III) by the CO_2 radical anion restores the Fe(II) state and produces CO_2 (**VII** to **VIII** to **I**).

Strong evidence suggests the methylphosphonate radical formed in **VII** (Scheme 3A) is a key mechanistic branch point that distinguishes the reactivity of *N. maritimus* MpnS and HEPD. While MpnS quenches the methylphosphonate radical by hydrogen transfer from formate, HEPD directs the transfer of the Fe(III)-bound hydroxyl to form hydroxymethylphosphonic acid **17** and formate as final products (Hirao & Morokuma, 2010, 2011; Peck et al., 2011; Whitteck et al., 2011). The variation of one of the facial-triad Fe(III) ligands, from glutamate to glutamine, plays a key role in this divergent reactivity. In the MpnS active site, the amide NH_2 of the Fe(III) coordinating ligand Gln152 is ideally located to provide a hydrogen bond to formate that is produced upon C—C bond cleavage (Born et al., 2017). It was proposed that by anchoring formate in proximity to the methylphosphonate radical, hydrogen transfer from formate to the radical is facilitated and **1** is produced (Scheme 4A). In the case of *Streptomyces viridochromogenes* HEPD, the corresponding Glu176 side chain bound to the Fe(III) ion cannot simultaneously anchor the formate with a hydrogen bond; thus this product is either released or rotated while bound to Fe(III), placing the formate hydrogen out of reach. Consequently, the methylphosphonate radical reacts with the Fe(III)-bound hydroxide

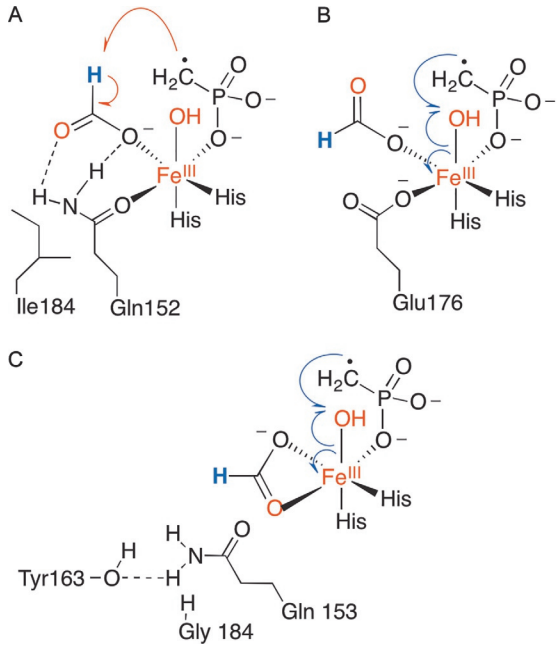

Scheme 4 The role of Fe(III) coordinating and second sphere amino acids side chains in directing the fate of a methylphosphonate radical in (A) *N. maritimus* MpnS, (B) *S. viridochromogenes* HEPD, and (C) *S. albus* HEPD.

producing **17** (Scheme 4B). It should be noted that a mechanistic variation of Scheme 4A and B involving transfer of hydride from formate, or hydroxide from Fe(II), to a methylphosphonate carbocation would also satisfy the current experimental data on MpnS and HEPD (Peck et al., 2017).

The presence of glutamine as a Fe(III) ligand is not sufficient in itself to confer MpnS activity. This is observed in a homologous enzyme from *Streptomyces albus* that, despite the presence of Gln153 as a Fe(III) ligand, has HEPD activity (Born et al., 2017). The structure of *S. albus* HEPD revealed an important role for a pair of second-sphere active site residues, Gly184 and Tyr163, with the former creating a space for Gln153 to release and rotate away from the Fe(III) ion, and the latter stabilizing this alternate conformation with a hydrogen bond (Scheme 4C). The mobility of Gln153 was proposed to allow formate to move away from the methylphosphonate radical and prevent hydrogen atom transfer. In the case of *N. maritimus* MpnS, the glycine is replaced by a bulky isoleucine side chain (Ile184), which sterically prevents Gln152 from rotating away from the Fe(III) ion (Scheme 4A). Gratifying support for the mobility hypothesis was obtained from the

conversion of *S. albus* HEPD to an equally active MpnS, with no residual HEPD activity, by substitution of the two second sphere residues to the *N. maritimus* MpnS counterparts (Y163F/G184I) (Born et al., 2017).

These experiments have thus identified a minimal sequence motif, glutamine as a facial-triad ligand for Fe(III), and isoleucine to anchor the glutamine ligand in place, that can accurately identify MpnS gene products from genome sequences. This led to the discovery and functional annotation of an MpnS from *Pelagibacter ubique* (Born et al., 2017). Unlike sequences encoding HEPD and HppE, which are found in marine and terrestrial bacteria, *mpnS* has only been detected so far in marine microorganisms. Surprisingly, *mpnS* sequences also appear in the eukaryotic genus Symbiodinium, a marine dinoflagellate. From Global Ocean Survey data, the *mpnS* sequence has been detected in 0.6% of marine microorganisms (Metcalf et al., 2012). While this may appear to be a low frequency, it is important to note that some of the genre captured in this value, such as *Pelagibacter* and *Nitrosopumilus*, are among the most commonly found organisms in the sea. This implies that the biosynthesis of **1** creates a substantial latent pool of methane.

The HppE reaction is profoundly different than that of HEPD or MpnS, despite a very similar active site architecture (Higgins et al., 2005). Unlike these enzymes, HppE does not incorporate molecular oxygen into products and instead functions as a dehydrogenase. Early studies proposed that HppE used molecular oxygen to extract two hydrogens and two electrons from *S*-2-hydroxypropylphosphonic acid **18** to form the epoxide ring in **3** (Higgins et al., 2005; Liu et al., 2001, 2003). The proposed catalytic cycle required an external source of two additional electrons to reduce O_2 to water (Yan, Munos, Liu, & Liu, 2006). However, more recently it was discovered that HppE can efficiently use hydrogen peroxide as an oxidant (Scheme 2C) (Wang et al., 2013). The proposed mechanism involves the oxidation of the Fe(II) nucleus by peroxide to form a ferryl species (Scheme 3B, **I** to **II**), which proceeds to remove the pro-*R*, C1 hydrogen and one electron from (*S*)-**18** (Hammerschmidt, 1991; Hammerschmidt & Kaehlig, 1991), thus restoring the iron nucleus to the Fe(II) state without the input of external electrons. The reactivity patterns of substrate analogs support the formation of a carbocation intermediate (**IV**) (Chang, Dey, et al., 2013; Chang, Mansoorabadi, & Liu, 2013; Woschek, Wuggenig, Peti, & Hammerschmidt, 2002). This carbocation is quenched by stereospecific attack of the adjacent C2 hydroxyl, forming the epoxide ring in **3**. When compared to MpnS and HEPD, HppE is notable for its apparent selectivity

for H_2O_2 over O_2 as an oxidant in order to access this reaction manifold. It is still not fully understood how this selectivity is achieved, or how H_2O_2 would be produced in the cell for HppE activity. The reader is encouraged to see the following reviews by Nair and van der Donk (2011) and Peck and van der Donk (2017) that include in depth discussions on the structures and mechanisms of MpnS, HEPD, and HppE.

1.3 Catabolism of Methylphosphonic Acid by Carbon–Phosphorus Lyase

1.3.1 Strategies for Cleaving C—P Bonds

Marine microorganisms are chronically starved for Pi. A common strategy used by microorganisms to survive under low Pi conditions is to derive this nutrient through catabolism of Pn, hypophosphite, and phosphite. As noted above, **1** and **2** occur frequently in the membranes, proteins, and glycans of marine microorganisms, thus providing a source of Pn. However, in order to extract Pi from Pn, specialized enzyme pathways are required that can cleave the C—P bond, which is notably resistant to cleavage by thermal, photochemical, and typical hydrolytic enzymes (e.g., phosphatases). Currently three enzyme mechanisms are known to cleave C—P bonds of Pn: (1) hydrolytic, as exemplified by the phosphonoacetaldehyde and phosphonoacetate hydrolases, (2) oxidative, by the nonheme Fe(II)-dependent oxygenases PhnY* and PhnZ, and (3) radical, by C—P lyase. These pathways were recently reviewed (Horsman & Zechel, 2017; Hove-Jensen, Zechel, & Jochimsen, 2014; Kamat & Raushel, 2013b). The C—P lyase reaction is notable for two reasons. First, while the hydrolytic and oxidative enzymes are substrate specific, C—P lyase is distinguished by its ability to release Pi from a wide structural range of Pn (Frost, Loo, Cordeiro, & Li, 1987; Parker, Higgins, Hawkes, & Robson, 1999; Wackett, Shames, Venditti, & Walsh, 1987), as well as organophosphinates (requiring cleavage of two C—P bonds) (Wackett, Shames, et al., 1987), and phosphite (requiring H—P bond cleavage) (Metcalf & Wanner, 1991). It is also the only enzyme system known to catabolize **1**. Second, C—P bond cleavage does not occur directly on **1**, but instead follows conjugation of **1** to a sugar as part of a multistep process called the C—P lyase pathway.

1.3.2 The phn *Operon*

In *E. coli*, the C—P lyase pathway is encoded by the *phn* operon and consists of 14 genes *phnCDEFGHIJKLMNOP* (Chen, Ye, Zhu, Wanner, & Walsh, 1990; Metcalf & Wanner, 1991, 1993b, 1993a). The *phn* operon is found

widely in bacterial genomes, including marine bacteria (Martinez, Ventouras, Wilson, Karl, & DeLong, 2013). Huang and colleagues have reviewed the considerable variation that is observed across species in the structure of the *phn* operon, which suggests that this sequence has undergone multiple horizontal gene transfer events, thereby highlighting the utility of this operon to bacterial survival (Huang, Su, & Xu, 2005). Using the strictly conserved *phnJ* sequence as a marker, Quinn and colleagues have identified 23% of sequenced marine bacterial genomes as containing *phn* operons (Villarreal-Chiu & Quinn, 2012). Accordingly, such bacteria have the potential to catabolize **1** into Pi and methane. Analysis of metagenomic DNA samples acquired by the Global Ocean Survey reveals a similar story, with 30% of the 83 sampled ocean sites testing positive for the *phn* operon (Villarreal-Chiu & Quinn, 2012). The *phnJ* sequence occurs in the equivalent of 5% of all marine genomes sampled by the Global Ocean Survey. Karl and colleagues observed a similar frequency of *phn* genes in metagenomic samples isolated from the Sargasso Sea (Karl et al., 2008). Such data point to a widespread microbial potential to produce methane from **1**. Indeed, in a milestone paper, Karl and colleagues demonstrated that seawater deprived of Pi but supplemented with **1** would produce methane (Karl et al., 2008). More recently, Repeta and colleagues estimated that daily C—P lyase-mediated turnover of only 0.2–0.3% of the marine reservoir of **1** would be sufficient to account for the methane paradox (Repeta et al., 2016).

DeLong and colleagues have exploited the ability of marine bacteria to survive Pi deprivation to select for genes encoding catabolism of Pn and other P sources. This has led to the discovery of the oxidative pathway encoded by *phnY*phnZ* (Martinez, Tyson, & DeLong, 2010) and the observation of widespread use of genes encoding enzymes for the acquisition and oxidation of phosphite (Martinez, Osburne, Sharma, DeLong, & Chisholm, 2012; Polyviou, Hitchcock, Baylay, Moore, & Bibby, 2015). The essential role of C—P lyase in catabolism of **1** by marine bacteria was demonstrated when **1** as a Pi source efficiently selected for bacterial species that possessed *phn* operons (Martinez et al., 2013). Similarly, when an *Escherichia coli phn* deletion strain was used to screen a fosmid library of marine metagenomic DNA for utilization of **1** as a Pi source, only fosmids with *phn* operons were selected (Martinez et al., 2013). However, in marine environments, microorganisms are more likely to encounter **1** and other Pn not as free molecules, but as esters with dissolved organic matter, such as polysaccharides (Repeta et al., 2016). Addressing this issue, Sosa and colleagues enriched bacteria from the Sulfitobacter and Oceanospirillaceae families by amending

seawater with polysaccharide-Pn esters obtained from dissolved organic matter (Sosa et al., 2017). In such polysaccharides, 20% of the total P content is represented by Pn (Repeta et al., 2016). The bacterial isolates produced methane from the polysaccharides, consistent with the action of C—P lyase on **1**, and *phn* operons were found in 20% of the sequenced genomes (Sosa et al., 2017). Surprisingly, these strains also produced ethylene from marine polysaccharide-Pn and free **8**, which is at odds with the radical mechanism of C—P lyase discussed below (Sosa et al., 2017). It is observed that *phn* operons are found throughout the water column at the ALOHA station, but the frequency peaks (1/200 genomes) where methane reaches supersaturation (125–200 m) (Sosa et al., 2017). Because C—P lyase cannot process esters of Pn, **1** and other Pn must be released from dissolved organic matter by an enzyme with phosphonate monoesterase activity, and indeed genes encoding such an enzyme appear to be present in the genomes of the *Sulfitobacter* isolates (Sosa et al., 2017). It is also noteworthy that the *phnO* sequence, encoding an aminoalkylphosphonate *N*-acetyltransferase (Errey & Blanchard, 2006), is absent from marine *phn* operons that have been selected this way. PhnO is used in C—P lyase pathways that catabolize aminoalkylphosphonates such as **2** (Hove-Jensen, McSorley, & Zechel, 2012); thus its absence is consistent with N-acetylation being a superfluous reaction for an organism that subsists on **1** as a Pi source.

The *phn* operon is a member of the phosphate (Pho) regulon and thus its expression is induced in response to Pi limitation (Wackett, Wanner, Venditti, & Walsh, 1987) (for reviews on the Pho regulon see Hsieh & Wanner, 2010; McGrath, Chin, & Quinn, 2013). The detection of environmental Pi levels is performed by seven membrane-associated proteins. Four of these proteins form the phosphate-specific transporter (Pst), which is the primary means for transporting Pi into the cell. Pst is an ABC-type membrane transport system consisting of a Pi-specific periplasmic binding protein PstS, a transmembrane component comprised of PstA and PstC, and an ATPase component PstB. Pst communicates with a two-component membrane system consisting of the membrane protein PhoR and the response regulator PhoB that controls expression of genes of the Pho regulon. Communication between Pst and PhoR/PhoB is mediated by an inhibitory protein PhoU: when Pi levels are low, PhoU ceases to inhibit PhoR/PhoB, leading to expression of the Pho regulon (Gardner, Johns, Tanner, & McCleary, 2014). A second level of control of the *phn* operon may be exerted by the *phnF* gene product, which encodes a transcriptional regulator. Although *phnF* is not strictly conserved in *phn* operons (Huang et al.,

2005), this sequence is observed in marine *phn* operons that encode the catabolism of **1** (Martinez et al., 2013). The *Mycobacterium smegmatis* PhnF binds to a DNA sequence between *phnF* and *phnD* and represses the transcription of the Pi transport operon, *phnDCE* when Pi levels are high (Gebhard et al., 2014; Gebhard & Cook, 2008). However, the ligand that releases PhnF from its repressor site is unknown.

In *E. coli* induction of expression of *phn* occurs when Pi concentrations fall below approximately 4 μ*M* (Hsieh & Wanner, 2010; Metcalf & Wanner, 1991; Wanner, 1993), a value that exceeds the maximal value found in most marine environments (Karl, 2014). Using measurements from the ALOHA station as an example (Karl, 2014), the Pi concentration varies from 50 to 200 n*M* in the eutrophic zone (0–200 m depth), then increases to 3 μ*M* for depths greater than 1000 m. For this reason, the *phn* operon is often actively expressed in marine bacteria, such as the cyanobacterium genus Trichodesmium (Dyhrman et al., 2006), which is widely found in tropical and subtropical oceans. In *E. coli*, the expression of the *phn* operon can be artificially rendered constitutive by deleting *pstS* (Hove-Jensen, Rosenkrantz, Zechel, & Willemoës, 2010). This has proven very useful for studying Pn catabolism by C—P lyase *in vivo* as Pi does not need to be omitted from the culture medium (Hove-Jensen et al., 2012; Hove-Jensen, McSorley, & Zechel, 2011).

1.3.3 Transport of Methylphosphonic Acid by PhnCDE

The beginning of the C—P lyase pathway for **1** involves transport into the bacterial cell. This is performed by PhnCDE, which comprises an ABC transporter where PhnD is a Pn periplasmic binding protein, PhnE is a transmembrane protein, and PhnC is an ATPase component (Scheme 1). In addition to association with the *phn* operon, the *phnCDE* sequence has been observed in microbial genomes either alone (Gebhard, Tran, & Cook, 2006; Martinez et al., 2012) or in association with gene clusters encoding different mechanisms of Pi utilization (Martinez et al., 2012). Differences in ligand specificities are observed between PhnD homologs from different bacterial species, likely reflecting recruitment of this transporter for different roles. This is demonstrated by Feingersch and colleagues who used ITC measurements to compare PhnD homologs (Feingersch et al., 2012). *E. coli* PhnD can effectively bind to **1** ($K_D = 18.4\,\mu M$), **2** (0.1 μ*M*), ethylphosphonic acid (1.4 μ*M*), aminomethylphosphonic acid (16.6 μ*M*), but not to Pi or phosphite. In contrast, the marine bacterial species *Prochlorococcus* MIT9301 has two transporters encoded by two separate loci, *ptxABCD* and *phnDCE*

(Martinez et al., 2012). Feingersch demonstrated that *Prochlorococcus* PtxB can bind to phosphite ($K_D = 2.0\,\mu M$), **1** ($0.8\,\mu M$), and ethylphosphonic acid ($2.8\,\mu M$) but not **2**. In contrast, *Prochlorococcus* PhnD can bind tightly to phosphite ($0.12\,\mu M$), **1** ($39\,\mu M$) and Pi ($54.9\,\mu M$), but not ethylphosphonic acid or **2** (Feingersch et al., 2012).

1.3.4 Ribosylation of Methylphosphonic Acid by PhnI(GHL)

The first committed step in the catabolism of **1** by C—P lyase involves a glycosyl transfer reaction by PhnI. Evidence of this reaction had been inferred by Avila, Draths, and Frost (1991) and by Hove-Jensen et al. (2011) from the observation of α-D-ribosyl-1-alkylphosphonates in cultures of *E. coli* grown on Pn, but the *phn* gene product that was responsible for this transformation was not known. The breakthrough occurred when Kamat and Raushel recognized that *E. coli* PhnI, a protein that had previously been shown by Jochimsen and colleagues as part of a PhnGHIJK protein complex (Jochimsen et al., 2011), had weak sequence similarity to nucleosidases (Kamat, Williams, & Raushel, 2011). Based on this clue, Kamat and Raushel were able to show that PhnI alone could catalyze the hydrolysis of GTP and ATP to form D-ribose-5-triphosphate **19** and the corresponding base (Scheme 5) (Kamat, Williams, et al., 2011). Hydrolysis was observed even in the presence of **1**. However, in combination with PhnG, PhnH, and PhnL, PhnI was shown to catalyze the transfer of ribose to **1** using GTP or ATP as glycosyl donors, forming **9** with inversion of anomeric stereochemical configuration. Therefore, a minimal set of proteins comprising

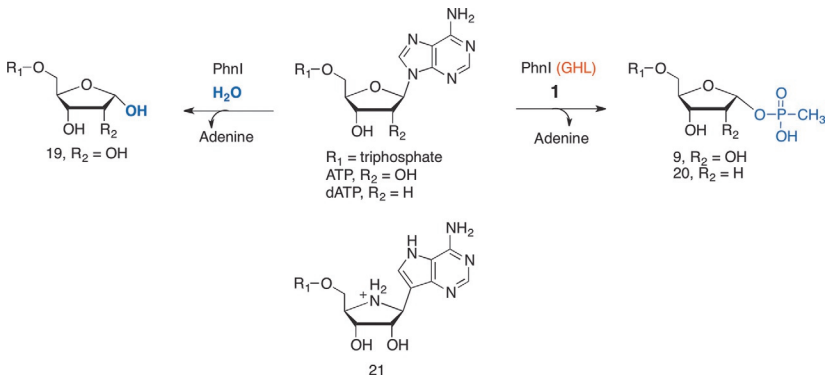

Scheme 5 Reaction of the carbon–phosphorus lyase component PhnI with nucleoside triphosphates either alone or in combination with PhnG, PhnH, and PhnL. The oxacarbenium ion transition state mimic **21** is a potent inhibitor of PhnI.

PhnG, PhnH, PhnI, and PhnL is essential to dictate the glycosyl acceptor specificity (H_2O or **1**) of PhnI. The PhnGHIL catalyzed reaction also accepts dATP as a donor for transfer to **1**, thereby forming the 2-deoxy analog **20** (Kamat, Williams, Dangott, Chakrabarti, & Raushel, 2013). The oxocarbenium ion transition state that is common to glycosyltransferase reactions is also stabilized by PhnI, as shown by the potent inhibition of PhnI by the transition state analog **21** ($K_I = 20\,nM$) (Kamat, Burgos, & Raushel, 2013) (Scheme 5). It is important to note that the PhnG, PhnH, PhnI, and PhnL polypeptides are unstable when reconstituted *in vitro*, which presented a unique challenge to reconstituting the PhnI reaction. In the experiment described above, the individual proteins require glutathione-*S*-transferase (GST) tags to enhance solubility. However, assembly and catalysis only occur upon removal of the GST tag *in situ* by addition of a protease, and even then, precipitation was observed during the course of the reaction (Kamat, Williams, et al., 2011).

1.3.5 Triphosphate Hydrolysis by PhnM

PhnM belongs to the amidohydrolase superfamily (Seibert & Raushel, 2005). Unlike the PhnG, PhnH, PhnI, and PhnL polypeptides described in the previous section, PhnM could be produced and purified from *E. coli* without a solubility tag. Kamat and Raushel demonstrated that PhnM catalyzes the hydrolysis of the α–β bond of the 5-triphosphate group of **9**, producing the 5-phosphate derivative **10** (Scheme 1) (Kamat, Williams, et al., 2011). Running the reaction in $H_2^{18}O$ produced **10** with ^{18}O incorporated into the 5-phosphate and not diphosphate; thus PhnM directs the hydrolytic water molecule toward the α-phosphate of **9**. *In vivo*, the 5-phosphoryl groups of **9** and **10** are sensitive to nonspecific phosphatase activity. If these intermediates accumulate in cells, one can observe the production of the shunt product α-D-ribosyl-1-methylphosphonate. Frost and colleagues were the first to indirectly observe the PhnI and PhnM reaction products by isolating α-D-ribosyl-1-ethylphosphonate from an *E. coli* mutant subsisting on ^{32}P-labeled ethylphosphonic acid (Avila et al., 1991). Likewise, Hove-Jensen and colleagues observed α-D-ribosyl-1-phosphite and several α-D-ribosyl-1-alkylphosphonates by ^{31}P NMR spectroscopy in cultures of *E. coli phnP* or *phnJ* deletion mutants, depending on the Pn source used in the experiment (Hove-Jensen et al., 2011, 2012). These shunt products are readily observed in culture supernatants by ^{31}P NMR spectroscopy because the signals appear far downfield (δ 13–30 ppm) in the spectra relative to more common biological phosphate esters and diesters.

1.3.6 C—P Bond Cleavage by PhnJ

A first clue into the identity of the intermediate that underwent C—P bond cleavage came from mutagenesis studies in *E. coli*. Hove-Jensen and colleagues observed by ^{31}P NMR spectroscopy that an *E. coli phnJ* deletion strain accumulated α-D-ribosyl-1-methylphosphonate when fed **1** as a Pi source, whereas the *phnP* deletion strain accumulated this compound plus α-D-ribosyl-1,2-cyclic phosphate (Hove-Jensen et al., 2011). These compounds correspond to the 5-phosphorylated intermediates **10** and **11** shown in Scheme 1. Intermediate **10** was proposed to be the substrate for C—P lyase, with C—P bond cleavage generating **11**. The latter was shown to be the substrate for the phosphodiesterase PhnP, discussed in the next section. Kamat and Raushel hypothesized that PhnJ was the enzyme that cleaved the C—P bond of **10** to form **11** and methane (Kamat, Williams, et al., 2011). Underpinning this hypothesis was the presence of four conserved cysteine residues in the PhnJ sequence, which suggested PhnJ might bind an iron–sulfur ([4Fe–4S]) cofactor. Such enzymes are well known to perform radical reactions (Broderick, Duffus, Duschene, & Shepard, 2014; Frey, Hegeman, & Ruzicka, 2008; Wang et al., 2014) and would explain the radical basis of the C—P lyase reaction that had been inferred over 20 years earlier by feeding Pn based radical probes to *E. coli* (Frost et al., 1987; Shames, Wackett, LaBarge, Kuczkowski, & Walsh, 1987).

Iron–sulfur cluster-dependent enzymes are highly sensitive to oxidation, which also proved to be the case with PhnJ. Kamat, Raushel, and colleagues were successful in producing and purifying GST tagged PhnJ from *E. coli* under aerobic conditions, yielding a black protein solution that contained 2 mol Fe ion per mol PhnJ (Kamat, Williams, et al., 2011). This was consistent with the presence of an oxidized and nonfunctional [4Fe–4S] cluster. After equilibrating the enzyme with Fe(II) and Na_2S under anaerobic conditions the PhnJ solution turned brown-red and had an absorbance spectrum consistent with a cluster in a $[4Fe–4S]^{2+}$ oxidation state. Upon reduction with dithionite, PhnJ had absorbance and EPR spectra that reflected a $[4Fe–4S]^{1+}$ oxidation state (Kamat, Williams, et al., 2013), which is the active form of the cofactor in radical *S*-adenosyl-L-methionine (SAM)-dependent enzymes. Kamat, Raushel, and colleagues demonstrated that PhnJ converts **10** to **11** in the presence of SAM **22**, with coproduction of methane, 5′-deoxyadenosine **24**, and L-methionine (Scheme 6) (Kamat, Williams, et al., 2011). The reaction proceeded only under anaerobic conditions and with the addition of dithionite. This is consistent with PhnJ using

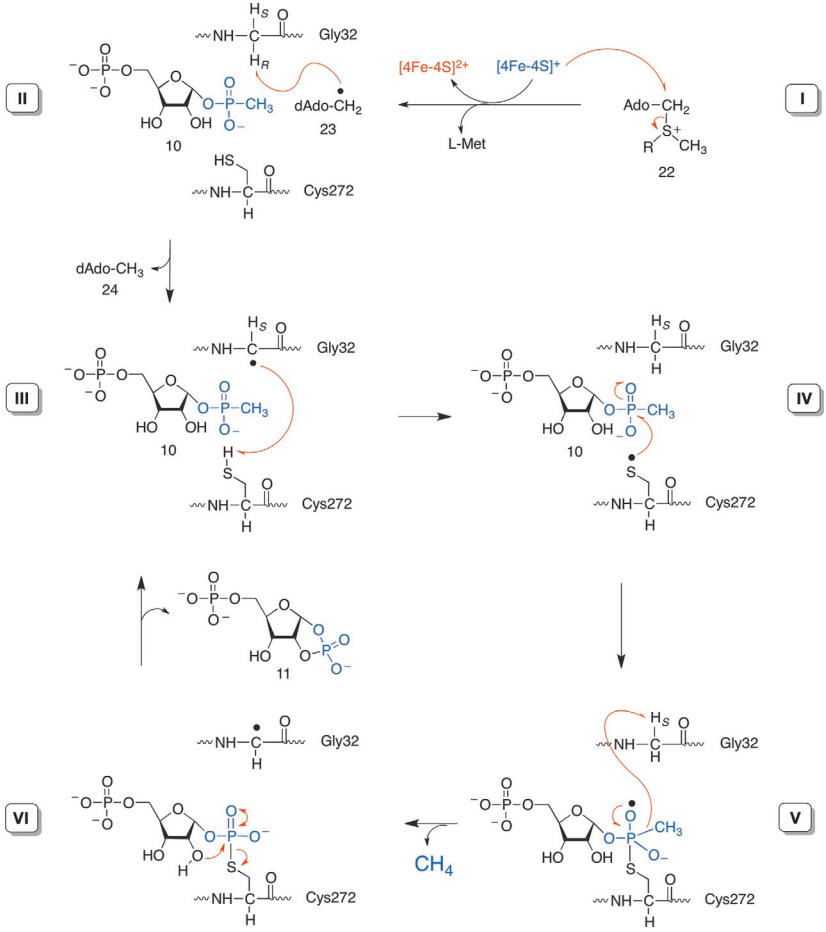

Scheme 6 Proposed mechanism for C—P bond cleavage by the PhnJ component of carbon–phosphorus lyase. *Ado*, adenosine; *dAdo*, 5′-deoxyadenosine.

a $[4Fe–4S]^{1+}$ cluster as a one electron donor to reductively cleave the 5′-C-S bond of SAM, yielding a 5′-deoxyadenosyl radical **23** (Scheme 6, **I** to **II**). Notably, PhnJ was inactive as the GST fusion; therefore this reaction, like that of PhnI supplemented with PhnG, PhnH, and PhnL described above, was initiated by removing the GST tag *in situ* with a protease. Precipitation of PhnJ and limited turnover suggests that this activity is unstable outside of the context of the PhnGHIJK protein complex described below. Nevertheless, reconstitution of the activity of PhnJ *in vitro* sets the stage for probing the mechanism of C—P bond cleavage.

A surprising aspect of PhnJ is that this enzyme represents a convergent evolutionary approach to forming a [4Fe–4S] cluster. Radical SAM-dependent enzymes typically use three conserved cysteine side chains to bind the [4Fe–4S] cluster (Shisler & Broderick, 2012). In contrast, PhnJ contains four conserved cysteine residues within the sequence $CX_2CX_{21}CX_5C$ (where X is any amino acid) that does not match the distinct CX_3CX_2C sequence found in the radical SAM superfamily of enzymes (Frey et al., 2008). Substitution of the four cysteines (Cys241, Cys244, Cys266, and Cys272) in PhnJ for alanine produced inactive PhnJ variants (Kamat, Williams, et al., 2013). However, PhnJ Cys272Ala could still form the [4Fe–4S] cofactor. Therefore, Cys272 appears to play a key role in catalysis, while the other three cysteines can be assigned roles in binding the [4Fe–4S] cluster.

A key question in the mechanism of PhnJ is how generation of the 5′-deoxyadenosyl radical **23** by the [4Fe–4S] cluster could initiate C—P bond cleavage. This was probed by determining the origin of the new hydrogen atoms in the reaction products 5′-deoxyadenosine **24** and methane. Deuterium was not incorporated into **24** when the PhnJ reaction was performed in D_2O, indicating that the hydrogen abstracted by **23** to form the 5′-methyl group of **24** does not originate from a solvent exchangeable position, either from within the PhnJ active site or from a substrate molecule. However, radical SAM enzymes are also known to use **23** to generate active site glycyl radicals, which are less reactive due to captodative stabilization of the radical by the neighboring α-amino and carbonyl groups (Broderick et al., 2014; Frey et al., 2008). To test this possibility, PhnJ was produced in *E. coli* grown in minimal medium supplemented with deuterated glycine ([2,2-$^2H_2$]-glycine), thereby replacing all the glycine residues with [2,2-$^2H_2$]-glycine. The reaction with [2,2-$^2H_2$]-glycine labeled PhnJ in H_2O produced **24** with a mass consistent with incorporation of a single deuterium atom in the 5′-methyl group. A single deuterium atom was also incorporated into methane by [2,2-$^2H_2$]-glycine labeled PhnJ, but only with a single turnover in H_2O; multiple turnovers led to unlabeled methane. Conversely, the reaction of unlabeled PhnJ in D_2O produced CDH_3. Overall this indicates that the new hydrogen in methane originates from a PhnJ glycine residue, but over multiple turnovers the glycine α-carbon hydrogens are acquired from the bulk solvent. Finally, by incorporating *R*- and *S*-deuterium-labeled glycine into PhnJ, it was determined that under single turnover conditions the pro-*R* hydrogen of a glycine residue is abstracted by **23**, and by inference, the pro-*S* hydrogen is incorporated into methane.

These experiments demonstrated that PhnJ is a glycyl radical SAM enzyme. Because *E. coli* PhnJ has eight glycine residues, the catalytic glycine

was first identified by running the PhnJ reaction for multiple turnovers in D_2O, which according to the previous experiments, must exchange the catalytic glycine hydrogens with deuterium (Kamat, Williams, et al., 2013). A single deuterium-labeled peptide was identified by LC–MS/MS analysis of protease-digested PhnJ, which contained the conserved glycine residue, Gly32. The corresponding PhnJ Gly32Ala variant was unable to cleave the C—P bond of **10** to produce methane, but still produced **24**. Moreover, running the reaction with PhnJ Gly32Ala labeled with L-[2,3,3,3-$^2H_4$]-alanine produced deuterium labeled **24**, demonstrating that Ala32 in the PhnJ Gly32Ala variant could still transfer a hydrogen atom to the radical **23**, but not transfer a hydrogen during C—P bond cleavage of **10** to produce methane. Overall, these experiments identified Gly32 as the site of glycyl radical formation in PhnJ.

With a sequence of hydrogen transfer events mapped within the active site of PhnJ, a mechanism for C—P bond cleavage can now be proposed (Scheme 6) (Kamat & Raushel, 2015). The PhnJ iron–sulfur cluster in the $[4Fe–4S]^{1+}$ oxidation state reductively cleaves SAM to form the 5′-deoxyadenosyl radical **23** and L-methionine (**I** to **II**). The catalytic cycle of PhnJ is initiated when **23** abstracts the pro-*R* hydrogen of Gly32 to form a glycyl radical and **24** (**II** to **III**). The glycyl radical is then proposed to abstract a hydrogen from Cys272 to form a thiyl radical (**III** to **IV**). Addition of the thiyl radical to the phosphorus center of **10** is thought to produce a phosphoranyl radical that promotes β-scission of the C—P bond (**IV** to **V**). The resulting methyl radical is then quenched by abstraction of the pro-*S* hydrogen of Gly32, forming methane (**V** to **VI**). It is important to note that early *in vivo* studies by Frost and colleagues revealed this step to be remarkably efficient (Frost et al., 1987); using cyclopropylmethylphosphonic acid as a "radical clock" substrate, abstraction of the PhnJ Gly32 pro-*S* hydrogen by the corresponding cyclopropylmethyl radical can be estimated to occur with rate constant of $6.5 \times 10^9 s^{-1}$. This high rate constant would be helpful in preventing inactivation of PhnJ by nonspecific hydrogen abstraction or addition reactions by the highly reactive methyl radical.

The C—P bond cleavage step (**V** to **VI**) predicts the formation of a covalent intermediate **VI** involving a phosphothioester linkage to Cys272. Turnover of this linkage is affected by intramolecular attack of the ribose 2-hydroxyl on the thioester, leading to α-D-ribosyl-1,2-cyclic phosphate **11** (**VI** to **III**). This step resets PhnJ for another round of catalysis. Preliminary evidence for covalent attachment of a phosphothioester intermediate **VI** to Cys272 has been observed by trapping PhnJ with a 2-deoxy analog of **10**,

which is unable to turn over due to the missing 2-hydroxyl (Kamat, Williams, et al., 2013). A ^{31}P NMR spectroscopic signal consistent with a phosphothioester linkage (δ 25 ppm) was observed on a proteolytically generated peptide from this sample, but the linkage was too labile to observe as an adduct by mass spectrometry.

1.3.7 Rescue of a Dead-End Intermediate by the Phosphodiesterases PhnP and PhnPP

An interesting feature of the PhnJ reaction is the production of 5-phospho-α-D-ribosyl-1,2-cyclic phosphate **11** as a product of C—P bond cleavage. Rather than evolving an ability to activate a water molecule to hydrolyze the phosphothioester intermediate, thereby directly forming metabolically useful α-D-ribosyl-1,5-bisphosphate **12** (Scheme 1), Nature opted to exploit the greater effective molarity of the adjacent ribose 2-hydroxyl. While this makes sense in terms of chemical reactivity, it does create a problem in that **11** is not immediately useful to the cell, and if it is not hydrolyzed to form **12** the cells will not survive. For this reason, hydrolysis of the 1,2-cyclic phosphate **11** is performed by a dedicated phosphodiesterase, either PhnP or PhnPP.

Metcalf and Wanner first identified *phnP* as the last essential gene of the *phn* operon through mutagenesis in *E. coli* (Metcalf & Wanner, 1993a). Later, Hove-Jensen and colleagues observed by ^{32}P radiolabeling and ^{31}P NMR spectroscopy that *E. coli phnP* deletion strains accumulated **10** and **11**, indicating that PhnP played a pathway specific role (Hove-Jensen et al., 2011, 2012). The *phnP* sequence encodes a hydrolase from the metal ion-dependent β-lactamase superfamily. Biochemical studies and X-ray crystallography revealed that PhnP uses a pair of manganese ions to activate water and the phosphoryl group to perform hydrolysis of a variety of phosphate diesters, but not monoesters (He et al., 2011; Podzelinska et al., 2009). *In vitro* PhnP will hydrolyze substituted methylphenylphosphates, *bis*(*p*-nitrophenyl) phosphate, and 2′,3′-cyclic nucleotides. Despite this broad substrate specificity, PhnP is highly specific toward the regioselective ring opening of the 1,2-cyclic phosphate of **11** to form **12** (Hove-Jensen et al., 2011). This reaction represented an important link to another C—P lyase component, PhnN, which had been previously shown by Hove-Jensen and colleagues to phosphorylate **12** to form 5-α-D-phosphoribosyl-1-pyrophosphate (PRPP) **16** (Hove-Jensen, Rosenkrantz, Haldimann, & Wanner, 2003).

In some *phn* operons, including those of marine bacteria (Martinez et al., 2013), the *phnP* sequence is replaced with a gene that encodes the cyclic

phosphate dihydrolase PhnPP. This enzyme is a member of polymerase and histidinol phosphatase subgroup of the amidohydrolase superfamily, and is variously annotated in databases and the literature as DUF1045 (Huang et al., 2005), *rcsF* (Martinez et al., 2013), or cog0613 (Ghodge, Cummings, Williams, & Raushel, 2013). Ghodge, Raushel, and colleagues demonstrated that PhnPP from *Eggerthella lenta* performed two successive hydrolysis reactions on **11**, first opening the 1,2-cyclic phosphate to form D-ribose-2,5-bisphosphate **13** (Scheme 1), followed by hydrolysis of the 2-phosphate to form D-ribose-5-phosphate **14** and Pi (Ghodge et al., 2013). The reaction of PhnPP with **11** is unusual in that it has the opposite regiospecificity relative to PhnP, and thus leads to another metabolic dead end in the form of **13**. The overall reaction is additionally novel in that PhnPP solves the problem posed by **13** with a specific phosphate monoesterase activity. Therefore, PhnPP is a rare example of an enzyme that has specific phosphate monoesterase and diesterase activities. In addition to releasing Pi for metabolic use, the product **14** can either enter the pentose phosphate pathway or be converted to **12** via isomerization by phosphopentose mutase (DeoB) followed by phosphorylation of the 5-hydroxyl of ribose. The latter reaction, however, has been ascertained only in archaeal species of the Thermococcales order (Aono, Sato, Imanaka, & Atomi, 2015).

1.3.8 Synthesis of PRPP by PhnN

The serendipitous discovery of the function of PhnN was the first unambiguous clue that C—P lyase was a pathway that fed into general metabolism. PhnN is an ATP-dependent kinase that converts the PhnP product **12** to PRPP **16** (Scheme 1). **16** is required by bacterial cells for the synthesis of pyrimidine and purine nucleotides, histidine, tryptophan, and NAD^+ (reviewed previously by Hove-Jensen et al., 2017; Jensen, Dandanell, Hove-Jensen, & Willemoes, 2008). Normally **16** is synthesized by the *prs* gene product, PRPP synthase. Hove-Jensen and colleagues attempted to select for mutations in an *E. coli prs* deletion strain that would relieve the requirement for supplemental NAD^+ (Hove-Jensen et al., 2003). Mutations were acquired within the *pst-phoU* operon that suppressed the NAD^+ requirement. It was previously known that mutations within this sequence, which control the Pho regulon, can lead to constitutive expression of the *phn* operon. This led to the determination that *phnN* could suppress the requirement for NAD^+ by *E. coli prs*, and thus play a redundant role in the cell. This was the first enzyme activity to be assigned to a *phn* gene product. As well, the structural similarity between **16** and α-D-ribosyl-1-ethylphosphonate,

discovered in *E. coli* over a decade earlier by Frost and colleagues (Avila et al., 1991), suggested C—P lyase performed catabolism of Pn through a catabolic pathway involving ribose.

1.3.9 Unknown Functions and the Phn(GHIJ)$_2$K Protein Complex

The functions of the C—P lyase components PhnG, PhnH, PhnK, and PhnL are either unknown or opaque. While PhnK and PhnL have sequences that resemble ATP binding proteins, reactions with this molecule or any nucleotide have yet to be demonstrated with these individual proteins. As noted previously, PhnL plays an important role in modifying the ribosyl acceptor specificity (H_2O or Pn) of the nucleosidase PhnI together with PhnG, PhnH, and PhnL (Kamat, Williams, et al., 2011). Complicating this picture is the observation that PhnG, PhnH, and PhnK are components of a larger, 240 kDa multiprotein complex with the composition Phn(GHIJ)$_2$K (Jochimsen et al., 2011; Ren et al., 2015; Seweryn et al., 2015). Jochimsen and colleagues demonstrated that this complex can be synthesized in soluble form in *E. coli* and purified either through multiple steps of ammonium sulfate precipitation, ion exchange chromatography, and size exclusion chromatography, or more conveniently in one step by Ni-NTA chromatography when PhnK has a C-terminal His$_6$ tag (Jochimsen et al., 2011). Smaller complexes comprised of PhnGI and PhnGHIJ can also be generated and purified by Ni-NTA chromatography (Jochimsen et al., 2011; Ren et al., 2015). Notably, expression of *phnL*, *phnM*, or any other *phn* gene is not required for assembly of Phn(GHIJ)$_2$K, nor do other polypeptides copurify with this complex. The Phn(GHIJ)$_2$K complex can also be observed in the gas phase when the complex is ionized under native conditions in ESI–MS (Ren et al., 2015). By raising the ionization and collisional energy of the MS instrument it was possible to observe the loss of each component of the Phn(GHIJ)$_2$K complex in the order PhnH–PhnI–PhnH–PhnI–PhnG–PhnI. PhnGI was the smallest fragment observed, suggesting that the overall complex is successively assembled by PhnGI and PhnHJ heterodimers (Scheme 7).

An X-ray crystal structure of a Phn(GHIJ)$_2$ protein complex, also designated the C—P lyase core complex, has been determined to 1.7 Å resolution (Scheme 7) (Seweryn et al., 2015). Overall the complex forms a two-fold symmetric octamer. The core of the complex is formed by homodimer of PhnI. Each PhnI in turn interacts with a copy of PhnG and PhnJ. The interaction between PhnI and PhnG is extensive, achieved by a β-hairpin and a C-terminal helix in PhnG that clamps onto a grove in PhnI.

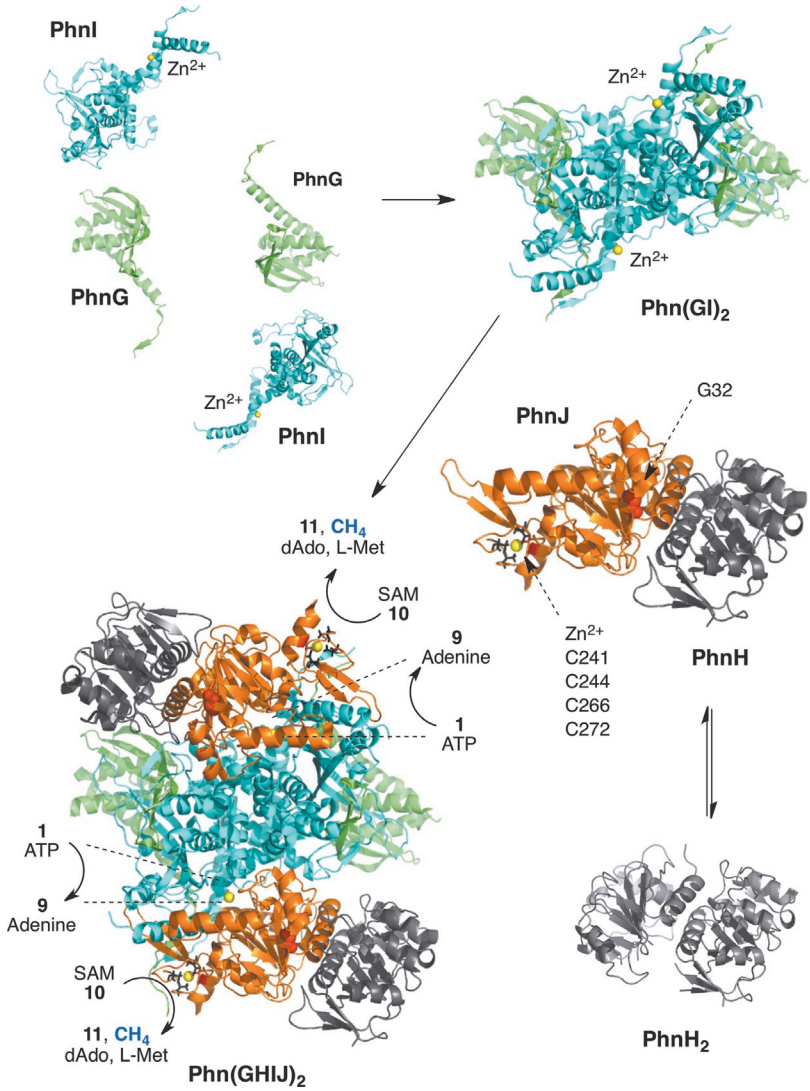

Scheme 7 Overview of the Phn(GHIJ)$_2$ core-complex (PDB ID: 4XB6) and its proposed assembly by the heterodimers PhnGI and PhnHJ. PhnH can also form a homodimer in solution. Putative active sites in PhnI and PhnJ are occupied by Zn^{2+} (*yellow spheres*). The [4Fe–FS] coordinating cysteine residues in the PhnJ active site are shown as *gray sticks* and the catalytic Cys272 is shown as *red sticks*. Note that a Zn^{2+} is observed in place of an intact [4Fe–FS] cluster. The catalytic Gly32 residue in PhnJ is shown as *red spheres*. Protein structures were rendered in PyMol (DeLano, 2002).

PhnI also has long N- and C-terminal helices that are used to bind a copy of PhnJ. A copy of PhnJ forms a reciprocal interaction with both copies of PhnI using an α-helical domain that has been labeled the central insertion domain. Finally, PhnH binds to the complex by forming a heterodimer with PhnJ, an interaction that is mediated by conserved α-helices in each protein. Notably, despite sharing little sequence similarity, the closest structural homolog to PhnH is PhnJ. The PhnHJ heterodimer is all the more intriguing when it is considered that PhnH alone will form a stable homodimer in solution utilizing the same α-helical interaction (Adams et al., 2008).

The location of the PhnI and PhnJ active sites has been tentatively identified in the Phn(GHIJ)$_2$ structure (Seweryn et al., 2015). A total of four sites are present, one for each copy of PhnI and PhnJ, each marked by a bound zinc ion. Because the [4Fe–4S] cluster of PhnJ was not reconstituted anaerobically prior to crystallization, a zinc ion is instead observed bound in each copy of PhnJ by Cys241, Cys244, Cys266, and Cys272. Three of these residues, Cys241, Cys244, and Cys266, are involved in binding the [4Fe–4S] cluster, while Cys272 is proposed form a covalent reaction intermediate during C—P bond cleavage (Scheme 6) (Kamat & Raushel, 2015). Surprisingly, Gly32, which transiently forms a glycyl radical and is proposed to abstract the hydrogen from the thiol side chain of Cys272, is found over 30 Å away from this residue. It is clear that a significant conformational change must occur to bring Gly32 and Cys272 together (within approximately 3 Å) to allow hydrogen atom transfer to occur. It is likely that a reactive conformation is achieved only when a functional [4Fe–4S] cluster is formed in the active site, or that the complex is capable of large conformational changes during catalysis.

The proposed active site of the glycosyltransferase PhnI is unusual in that it is partially formed by PhnJ. The active site appears at the end of a tunnel that leads to the surface of the Phn(GHIJ)$_2$ complex, and substrate access may be controlled by the central insertion domain of PhnJ. A zinc ion is observed bound in this cavity by His328 and His333 of PhnI while a third ligand, His108 is donated by PhnJ. Because Zn^{2+} typically prefers a tetrahedral coordination state, one ligand site is available to form a Lewis acid interaction with a substrate molecule. Substitution of any of the Zn^{2+} coordinating histidine side chains for alanine creates an inactive C—P lyase pathway *in vivo*, thereby confirming the importance of this site to overall pathway function (Seweryn et al., 2015). However, what must be reconciled is the observation that *in vitro* PhnI requires PhnG, H, and L for catalysis (Scheme 5), but not PhnJ. Additionally, while PhnI is observed to interact directly with PhnG in the Phn(GHIJ)$_2$ protein complex (and can be copurified as a PhnGI

complex), no direct interaction is observed with PhnH. Finally, PhnL must only transiently visit PhnI during catalysis as this protein does not copurify as part of any complex.

The symmetry of the Phn(GHIJ)$_2$ complex is disrupted by PhnK. While PhnK could not be crystallized with PhnGHIJ despite copurifying with this complex, a single copy of PhnK has been observed bound to Phn(GHIJ)$_2$ using negative stain electron microscopy (Seweryn et al., 2015) and single particle cryoelectron microscopy (Yang, Ren, Raushel, & Zhang, 2016). PhnK binds to the central insertion domain of PhnJ. While two identical PhnK binding sites are available on the Phn(GHIJ)$_2$ complex, only a single copy of PhnK can bind due to steric interference with the second binding site (Yang et al., 2016). This raises the possibility that PhnK exerts an allosteric effect and may induce the Phn(GHIJ)$_2$ protein complex to have half-site reactivity (Bernhard & MacQuarrie, 1973), where only one PhnJ and PhnI active site is available for catalysis in a given cycle. Adding significance and intrigue to the allosteric hypothesis is the exposure of the PhnJ active site residue Gly32 to solvent when bound to PhnK (Yang et al., 2016). In the unbound copy of PhnJ, Gly32 remains buried, and presumably unavailable for catalysis.

1.4 Rationale for the Chosen Protocols

MpnS and C—P lyase are the focus of the following protocols as they represent unique and key transformations that lead to and from **1**. MpnS and C—P lyase both catalyze novel bond cleavage reactions (C—C and C—P) that offer opportunities to study the activation of molecular oxygen by iron, the reactivity of radical intermediates, and the role of multiprotein complexes in enzyme catalysis. Accordingly, these protocols offer a starting point to the investigator who is interested in studying these and related enzymes, and provide greater detail on nuanced, but critical, steps that are often abbreviated in the literature and assume prior expertise.

2. METHYLPHOSPHONIC ACID SYNTHASE

2.1 Heterologous Expression and Purification of MpnS

The *mpnS* gene from *N. maritimus* has been expressed in *E. coli* using several different methods. A typical expression involves induction with 0.5 m*M* isopropyl-β-D-thiogalactopyranoside (IPTG) and incubation for 5 h at 30°C, followed by cooling the cells for 10 min before harvesting (Metcalf et al., 2012). The method outlined below was described previously (Born et al., 2017).

2.1.1 Equipment

- Sterilization facilities
- Incubator with thermostat and shaking device
- Spectrophotometer for optical density (OD) measurement at 600 nm
- French pressure cell (Thermo Electron Corporation)
- Nickel-nitrilotriacetic acid (Ni-NTA) agarose resin (Qiagen)
- Amicon Ultra centrifugal filters (EMD Millipore)
- NanoDrop spectrophotometer (Thermo Scientific)
- PD10 columns (GE Healthcare)
- Äkta FPLC system (GE Healthcare)
- Superdex 200 preparative grade resin (GE Healthcare)
- SDS-PAGE apparatus

2.1.2 Materials and Reagents

- *E. coli* Rosetta 2 (DE3) pLysS cells for expression (other BL21 strains may work as well, but these have not been tested)
- IPTG
- LB
- Ampicillin
- Chloramphenicol
- DNase
- Lysozyme
- 50 m*M* HEPES pH 7.5, 200 m*M* KCl, 20 m*M* imidazole, 10% (v/v) glycerol
- 50 m*M* HEPES pH 7.5, 200 m*M* KCl, 50 m*M* imidazole, 10% (v/v) glycerol
- 50 m*M* HEPES pH 7.5, 200 m*M* KCl, 250 m*M* imidazole, 10% (v/v) glycerol
- 50 m*M* HEPES pH 7.5, 200 m*M* KCl, 10% (v/v) glycerol

2.1.3 Protocol

1. Grow *E. coli* Rosetta 2 (DE3) pLysS cells (Novagen) harboring the pET-15b-*mpnS* plasmid in LB medium supplemented with 100 μg/mL ampicillin and 12.5 μg/mL chloramphenicol while shaking (200 rpm) at 37°C until an OD_{600} of 0.6–0.8 is reached.
2. Place the culture flasks in an ice water bath for 10 min before addition of IPTG to a final concentration of 0.1 m*M*. Incubate the cultures for 10–12 h while shaking (200 rpm) at 18°C.

3. Harvest the cells by centrifugation, and wash the pellets with 25 m*M* HEPES pH 7.5 before resuspension in lysis buffer (50 m*M* HEPES pH 7.5, 200 m*M* KCl, 20 m*M* imidazole, 10% (v/v) glycerol).
4. Incubate the resuspended cells with lysozyme (1 mg/mL) and DNase (0.01 mg/mL) at 4°C for 30 min before two passages through a chilled French pressure cell (Thermo Electron Corporation). Remove the cell debris by centrifugation at 35,000 × *g* for 1 h before protein purification by Ni-NTA chromatography at 4°C.
5. Incubate the supernatant with Ni-NTA resin equilibrated with 10 column volumes of lysis buffer (2.5 mL of resin per L of expression culture) for 30 min before collecting the flow-through. Wash the resin twice with 10 column volumes of wash buffer (50 m*M* HEPES pH 7.5, 200 m*M* KCl, 50 m*M* imidazole, 10% (v/v) glycerol). Elute the protein with elution buffer (50 m*M* HEPES pH 7.5, 200 m*M* KCl, 250 m*M* imidazole, 10% (v/v) glycerol).
6. Pool one column volume fractions based on absorbance at 280 nm measured by a NanoDrop spectrophotometer (Thermo Scientific). Concentrate the protein to approximately 2 mL using an Amicon Ultra centrifugal filter with a 30 kDa molecular weight cut off. Finally, desalt the protein solution using a PD10 column equilibrated with storage buffer (50 m*M* HEPES pH 7.5, 200 m*M* KCl, 10% (v/v) glycerol).
7. Assess the purity by SDS-PAGE, and measure the concentration by absorbance at 280 nm using a NanoDrop spectrophotometer with a theoretical extinction coefficient of 64,540 M^{-1} cm^{-1} calculated using the SIB ExPASy Bioinformatics Resources Portal (Artimo et al., 2012; Born et al., 2017). The typical yield is about 18 mg of protein per L of *E. coli* culture.
8. Store the final *N*-terminal His_6 fusion protein at −80°C in aliquots.
9. Additionally, the enzyme can be purified further by size exclusion chromatography using Superdex 200 preparative grade resin (GE Healthcare) equilibrated with at least two column volumes of storage buffer on an Äkta FPLC.

2.2 Assaying MpnS Activity With 2-Hydroxyethylphosphonic Acid

The conversion of **8** to **1** and CO_2 by MpnS can be readily monitored by ^{31}P NMR spectroscopy. The activity assay for MpnS has been described previously (Cooke et al., 2012).

2.2.1 Equipment

- NMR spectrometer with a ^{31}P probe
- Anaerobic chamber with an atmosphere of 97% N_2/3% H_2 (Coy Laboratory Products)

2.2.2 Materials and Reagents

- Reaction buffer: 50 m*M* HEPES pH 7.5
- ammonium iron(II) sulfate hexahydrate
- **8**, synthesized as previously described (Metcalf et al., 2012)
- MpnS stock solution
- **1** as a synthetic standard (Sigma-Aldrich)
- Chelex® 100 sodium form (Sigma-Aldrich)
- Amicon Ultra centrifugal filters (EMD Millipore)
- D_2O

2.2.3 Protocol

1. Reconstitute MpnS (100 μ*M* final concentration) in an anaerobic chamber (Coy Laboratory Products) with an atmosphere of 97%/3% N_2/H_2 with 1 *M* equivalent of $Fe(NH_4)_2(SO_4)_2$ in 50 m*M* HEPES pH 7.5 with incubation for 10 min on ice.
2. Set up an assay (500 μL) aerobically, which typically contains 10 μ*M* enzyme and 2 m*M* **8** in 50 m*M* HEPES pH 7.5. Incubate for 2 h at room temperature.
3. Incubate the reaction mixture with Chelex® for 20 min while shaking, and remove the protein using a Millipore centrifuge filter with a 30 kDa molecular weight cut off.
4. Add D_2O (100 μL, 20% final v/v) before analysis by ^{31}P NMR spectroscopy with ^{1}H decoupling. The observed chemical shifts of **8** and **1** are approximately δ 18 and 21–24 ppm, respectively. Because Pn chemical shifts are sensitive to pH around their pK_a values, product identity is confirmed by spiking with a synthetic standard of **1**. Under these conditions, the reaction is observed to have run to completion.

2.3 Kinetic Characterization of MpnS

The rate of oxidation of **8** to **1** and CO_2 by MpnS can be followed by monitoring the consumption of molecular oxygen. Experiments to measure oxygen consumption are performed on a Clark-type oxygen electrode. This assay method has been described previously by Cooke and colleagues (Cooke et al., 2012).

2.3.1 Equipment

- Clark-type oxygen electrode (Hansatech)
- Anaerobic chamber with an atmosphere of 97% N_2/3% H_2 (Coy Laboratory Products)

2.3.2 Materials and Reagents

- Reaction buffer: 50 m*M* HEPES pH 7.5
- ammonium iron(II) sulfate hexahydrate
- **8**, synthesized as previously described (Metcalf et al., 2012)
- MpnS stock solution

2.3.3 Protocol

1. Reconstitute MpnS with Fe(II) as described in Section 2.2.3. Reactions for the oxygen electrode (1 mL) typically contain 2 μ*M* MpnS and varying concentrations of **8** in 50 m*M* HEPES pH 7.5. Assays to measure k_{cat} and apparent K_M with respect to **8** are performed at air-saturated oxygen levels at 20°C.
2. Initiate reactions with substrate, and perform experiments in triplicate for each concentration of **8**. Measure the initial rate of oxygen consumption using the OxyGraph Plus software. With **8** as substrate, MpnS has an apparent $K_{M(8)}$ of 4.5 ± 1.1 μ*M*, k_{cat} of $0.18 \pm 0.01\ s^{-1}$, and catalytic efficiency of $(4.0 \pm 1.0) \times 10^4\ M^{-1}\ s^{-1}$.

2.3.4 Notes

Analysis of kinetic parameters with 2-[2-$^2H_2$]-**8**, (*R*)-[2-$^2H_2$]-**8**, and (*S*)-[2-$^2H_2$]-**8** has also been examined to gain insight on the timing of hydrogen atom abstraction, but no significant effect on k_{cat} was observed (Cooke et al., 2012). A slight increase in $K_{M(8)}$ was observed, but given the low $K_{M(8)}$ value for MpnS, it should be noted that experiments with substrate concentrations in the low μ*M* range are difficult due to the detection sensitivity of the oxygen electrode.

3. CARBON–PHOSPHORUS LYASE PATHWAY

3.1 Analysis of C—P Lyase Pathway Reaction Intermediates

The structure and quantification of the intermediates of the C—P lyase pathway have been studied primarily by two methodologies, ^{31}P NMR spectroscopy (Hove-Jensen et al., 2011) and radiolabeling by $^{32}P_i$ (Hove-Jensen et al., 2010).

3.1.1 ^{31}P NMR Spectroscopy

^{31}P NMR spectroscopy is a versatile methodology for the study of chemical reactions involving phosphorus-containing compounds. Chemical shifts of phosphate esters are relatively close to that of P_i, which is usually defined as 0.0. For example, the chemical shift (δ) of α-D-ribosyl 1-phosphate is δ 2–3 ppm and that of D-ribose-5-phosphate is approximately δ 4 ppm. Contrary to this, chemical shifts of Pn are located further downfield, i.e., with a much more positive value. For example, the signal for **1** is observed around δ 21–24 ppm. ^{31}P NMR spectroscopy greatly facilitated resolving the structure of the intermediates of the *E. coli* C—P lyase pathway. Also useful is the application of mutant strain defective in the *phnP* gene specifying phosphoribosyl cyclic phosphodiesterase. This mutant, also constitutive for expression of the remaining cistrons of the *phn* operon, accumulates not only the PhnP substrate **11** but also most of the intermediates prior to this compound. The accumulation of an intermediate furthermore causes excretion of the compound in dephosphorylated form (e.g., **11** yields α-D-ribosyl-1,2-cyclic phosphate). Chemical shifts commonly depend on solution pH, concentration, solvent, and the presence of other compounds. These factors may change the ^{31}P NMR chemical shifts by 1 ppm or greater.

3.1.1.1 Equipment

- Sterilization facility such as an autoclave
- Sterile toothpicks
- Sterile 10 mL glass or plastic tubes with caps
- Sterile 50 mL glass flasks
- Incubator with thermostat and shaking device
- Spectrophotometer for OD measurement at 436 or 600 nm. An OD of 1 (1 cm-light path) corresponds to approximately 6×10^{11} cells per L.
- Centrifuge tubes for 10 mL
- Centrifuge with rotor for 10 mL tubes
- Filtration unit for 47 mm-diameter filters (Thermo Scientific Nalgene)
- Capillary tubes for external standard in ^{31}P NMR spectroscopy
- NMR spectroscopy tubes (5 mm i.d.)
- NMR spectrometer equipped with a ^{31}P probe

3.1.1.2 Buffers and Reagents

- Growth medium, 03P. This medium contains per liter: Tris/HCl, 6.0 g; KCl, 2.0 g; NH_4Cl, 2.0 g; $MgCl_2$ (7 H_2O), 0.5 g; Na_2SO_4, 0.05 g;

0.15 *M* Na_2HPO_4, 2.0 mL; 10 m*M* $FeCl_3$, 1.0 mL. The pH is adjusted to 7.6 with HCl prior to sterilization by filtration (0.22 μm filter) or by autoclaving.
- Sterile glucose solutions, 2% and 20%
- Phosphoric acid, 85% or 17 m*M* as external standard
- Methylphosphonic acid **1**, 0.2 *M* in water, sterilized by filtration
- Whatman nylon membrane filters, pore size 0.45 μm, diameter 47 mm

3.1.1.3 Protocol

1. To a capped 10 mL incubation tube, add aseptically 2 mL of 03P medium and 20 μL 2% glucose. Inoculate aseptically the bacterial strain with a toothpick and incubate the tube overnight (15–20 h) at 37°C with shaking.
2. Add aseptically to a 50 mL flask 15 mL of 03P medium, 150 μL of 20% glucose and prewarm the flask at 37°C.
3. Assure growth (visualized as turbidity) in the overnight culture. Add 0.3 mL of the overnight culture to the flask and incubate at 37°C with shaking. Follow OD.
4. At an OD_{600} of approximately 0.45, add **1** to a final concentration of 2 m*M*. Continue incubation with shaking at 37°C.
5. After 5 h remove cells by centrifugation, and pass the supernatant fluid through a 0.45-μm filter. Analyze or store the filtrate at −20°C.
6. Add an appropriate volume of the filtrate to an NMR spectroscopy tube and submit to the NMR spectrometer.

3.1.1.4 Notes

Interpretation of ^{31}P NMR spectra is often, but not always, straightforward when spectra are run with proton decoupling, which results in one sharp peak per phosphorus nucleus. Fig. 3A shows the ^{31}P NMR spectrum obtained after growth of an *E. coli phnP* strain in the presence of 2 m*M* **1** as described above. The chemical shifts at δ 26.4 (indicated by an asterisk), 23.9, and 18.6 ppm correspond to α-D-ribosyl-1-methylphosphonate, **1**, and α-D-ribosyl-1,2-cyclic phosphate, respectively. The chemical shifts of the various phosphorus nuclei of the intermediates of the C—P lyase pathway catabolizing **1** are recorded in Table 1. As previously mentioned, chemical shifts may vary up to 1 ppm by alterations in pH or other conditions. Similarly, the chemical shifts of C—P lyase pathway intermediates for substrates other than **1** will vary from those listed in Table 1.

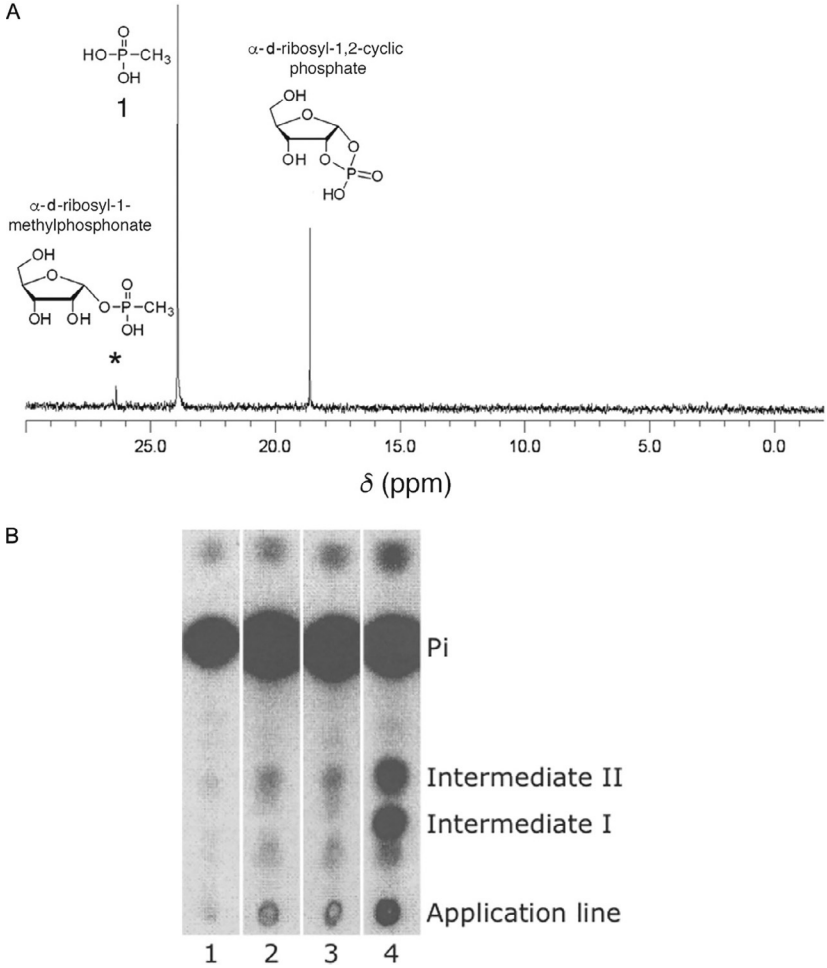

Fig. 3 Analysis of C—P lyase pathway intermediates by ^{31}P NMR and radiolabeling analyses. (A) ^{31}P NMR spectrum of the used medium after growth of strain HO2542 (*ΔphnP pstS*) in the presence of **1** (2 m*M*) for 5 h. The spectrum was obtained with proton decoupling in a Bruker Avance 400 MHz spectrometer (Hove-Jensen et al., 2011). The asterisk (*) marks the signal for α-D-ribosyl-1-methylphosphonate. (B) TLC of cultures of a *Δphn* strain (HO2680, lane 1), a *ΔphnH* strain (HO2534, lane 2), a *ΔphnN* strain (HO2540, lane 3), and a *ΔphnP* strain (HO2542, lane 4) grown in the presence of **1** and analyzed as described in the text (Hove-Jensen et al., 2010). *Panel (A) adapted with permission from the American Chemical Society. Panel (B) adapted with permission from the American Society for Microbiology and the American Chemical Society.*

Table 1 ^{31}P NMR Spectroscopic Chemical Shifts for Compounds of **1** Catabolism[a]

	Chemical Shift (δ, ppm)				
Compound	**C-Bound P**	**Ribosyl-1-P**	**Ribosyl-1,2-P**	**Ribosyl-2-P**	**Ribose-5-P**
1	23.9				
9	17.8				−2.9, −8.4, −17.6[b]
10	19.7				6.8
11			18.7		4.1
12		3.0			4.5
13				4.5	4.5
14					4.6
15		1.9			

[a]^{31}P NMR chemical shifts of Pn are sensitive to solvent and pH, which may result in small variations between spectra of the same compound. Chemical shift values were published previously (Ghodge et al., 2013; Hove-Jensen et al., 2011, 2012; Kamat, Williams, et al., 2011).
[b]Values represent chemical shifts of P of γ-, α-, and β-phosphoryl groups, respectively.

3.1.2 Radiolabeling by $^{32}P_i$

For identification and quantification of certain C—P lyase pathway intermediates, radiolabeling is a powerful methodology (K. Randerath & Randerath, 1966). $^{32}P_i$ may be replaced by $^{33}P_i$ although the latter has not previously been applied in this field. Both radioisotopes, ^{32}P and ^{33}P, are β-emitters with energies of 1.71 and 0.25 MeV, respectively, and with half-lives 14.3 and 25.4 days, respectively. Special safety precautions are necessary when working with radioisotopes.

3.1.2.1 Equipment

- Sterilization facility such as an autoclave
- Sterile toothpicks
- Sterile 10 mL glass or plastic tubes with caps
- Sterile 50 mL glass flasks
- Incubator with thermostat and shaking device and protection from radiation such as a metal, glass or Plexiglas lid.
- Spectrophotometer as described in Section 3.1.1.1
- Liquid scintillation vials, 20 mL
- Polyethyleneimine-coated cellulose on plastic sheets, 20 × 20 cm, for thin-layer chromatography (Baker-flex, J. T. Baker, Griesheim, Germany) or prepared as previously described (Hove-Jensen et al., 2011)

- Microfuge tubes, 1.5 mL
- Centrifuge with cooling for 1.5 mL microfuge tube
- Chromatography tanks
- Radioisotope detection, imaging and quantification equipment such as the Cyclone Storage Phosphor System (Perkin Elmer) with exposure of Storage Phosphor Screens

3.1.2.2 Materials and Reagents

- Growth medium, 03P, prepared as described in Section 3.1.1.2
- Sterile glucose solutions, 2% and 20%
- Methylphosphonic acid **1** (Sigma-Aldrich 289,868), 0.2 *M* in water
- Carrier-free $^{32}P_i$ (Nex-053, Perkin Elmer Life and Analytical Sciences, Waltham, MA)
- Formic acid, 2 *M*
- Methanol
- Acetic acid, 1 *M*
- LiCl, 3 *M*
- Solvent A prepared by mixing 50 mL 3 *M* LiCl and 450 mL 1 *M* acetic acid

3.1.2.3 Protocol

1. To a capped 10 mL incubation tube add aseptically 2 mL of 03P medium and 20 μL 2% glucose. Using a toothpick inoculate the medium aseptically with the bacterial strain to be analyzed and incubate the tube overnight (15–20 h) at 37°C with shaking.
2. Add aseptically to a 50 mL flask 20 mL of 03P medium and 200 μL of 20% glucose. Pre-warm the flask at 37°C.
3. Assure growth (visualized as turbidity) in the overnight culture. Add 0.4 mL of the overnight culture to the 50 mL flask and incubate at 37°C with shaking. Follow the OD.
4. Add 0.74 MBq of $^{32}P_i$ (e.g., 20 μL of a 1 mCi per mL solution) to the scintillation vial and prewarm at 37°C.
5. After one doubling of OD, transfer 2 mL of culture to the ^{32}P-containing scintillation vial, mix carefully, and continue incubation. Only follow the OD of the unlabeled culture in the 50 mL flask.
6. Follow OD in the unlabeled culture in the 50 mL flask throughout the entire experiment. After one additional doubling of OD, add **1** to a final concentration of 2 m*M* to both the unlabeled and the labeled cultures (20 μL of 0.2 *M* **1** to the radiolabeled culture). Mix carefully.

7. After an appropriate time of incubation, for example 4, 6, or 8 h, transfer 200 μL of the radiolabeled culture to a 1.5 mL microfuge tube precooled in ice and containing 40 μL of 2 *M* formic acid. Cap the tube, vortex for 30 s, then cool on ice for 20 min.
8. Centrifuge at 20,000 × *g* for 10 min and remove supernatant fluid to fresh cold microfuge tube. Freeze at −20°C or analyze by TLC.
9. For TLC apply slowly and carefully 10 μL of the supernatant fluid to a polyethyleneimine-coated cellulose TLC sheet and dry.
10. Develop the TLC sheet in methanol to the application line, followed by 1 *M* acetic acid (additional 2 cm), and solvent A (additional 15 cm), and dry.
11. Submit to imaging and quantification technology by the Phosphor Storage System.

3.1.2.4 Notes

The results of an analysis of accumulation of C—P lyase pathway intermediates of various *E. coli phn* mutant strains grown in the presence of **1** are shown in Fig. 3B. The structure of the compounds cannot be inferred from this analysis, but the compound labeled "Intermediate I" was shown to be the substrate **11** for *phnP*-specified phosphoribosyl cyclic phosphodiesterase (Hove-Jensen et al., 2011, 2012). However, the radiolabeling of intermediates permits the detection and calculation of the amount of compounds present in very small amounts. By the method described above compounds located in the medium as well as compounds located inside the cells are extracted. The method, thus, can be altered to determine only compounds in the growth medium (i.e., excreted compounds), by omitting the formic acid extraction of the culture, and, rather centrifugation of the culture and storage and analysis of the supernatant fluid. Analysis of intracellular material can be achieved by removing the growth medium by centrifugation, and extraction of the cell pellet with 240 μL of 0.33 *M* formic acid.

3.1.3 Isolation of C—P Lyase Pathway Intermediates

Several of the intermediates of the C—P lyase pathway have been isolated from cultures of *E. coli* cells grown in the presence of various Pn (Avila et al., 1991; Hove-Jensen et al., 2011; Kamat, Williams, et al., 2011). Other intermediates have been synthesized *in vitro* (Sections 3.4.4 and 3.5.2) (Avila et al., 1991; Hove-Jensen et al., 2011). The protocol described below takes advantage on the use of an *E. coli phnP* mutant strain, which is defective in phosphoribosyl cyclic phosphodiesterase. This mutant strain accumulates not only the substrate of the defective enzyme,

5-phospho-α-D-ribosyl-1,2-cyclic phosphate **11**, but also substrates of enzyme activities functioning prior in the pathway. In addition, the accumulation of an intermediate may cause excretion to the growth medium of the intermediate with simultaneous removal of the phosphate ester. The following protocol describes the isolation of compounds produced by the C—P lyase pathway of cells of strain HO2542 (*ΔphnP ΔpstS*) grown in the presence of **2**. The procedure is applicable to cells grown in the presence of **1** as well.

3.1.3.1 Equipment

- Sterilization facility such as an autoclave
- Sterile streaking needle
- Sterile 100 mL and 2 L glass flasks
- Incubator with thermostat and shaking device
- Spectrophotometer as described in Section 3.1.1.1
- AG1-X8 anion exchange resin, analytical grade, 100–200 mesh (BioRad) packed in a 2.5 × 30 cm column
- Centrifuge tubes for 40 mL or larger
- Centrifuge
- Filtration unit for 47 mm-diameter filters (Thermo Scientific Nalgene)
- Whatman nylon membrane filters, pore size 0.45 μm, diameter 47 mm
- Capillary tubes containing 17 m*M* phosphoric acid for external standard
- NMR spectroscopy tubes
- NMR spectrometer equipped with a ^{31}P probe
- Freeze dryer
- Äkta FPLC system (GE Healthcare)

3.1.3.2 Materials and Reagents

- Growth medium, 03P, prepared as described in Section 3.1.1.2
- Sterile glucose solutions, 2% and 20%
- Methylphosphonic acid **1**, 0.2 *M* in water, sterilized by filtration
- 4 *M* ammonium formate in 0.1 *M* formic acid
- 0.1 *M* formic acid
- Deionized water

3.1.3.3 Protocol

1. To a 100 mL sterile flask, add aseptically 20 mL of 03P medium and 200 μL 2% glucose. Inoculate aseptically the bacterial strain to be analyzed with a streaking needle and incubate the flask overnight (15–20 h) at 37°C with shaking.

2. Add aseptically to a 2 L flask 230 mL of 03P medium, 2.5 mL of 20% glucose and prewarm the flask at 37°C.
3. Assure growth (visualized as turbidity) in the overnight culture. Add 20 mL of the overnight culture to the 250 mL fresh medium and incubate at 37°C with shaking. Follow OD.
4. At an OD_{600} of approximately 0.5, add 2.5 mL of 0.2 *M* **1**. Continue incubation with shaking at 37°C for 24 h.
5. Remove the cells by centrifugation (Sorvall SS-34 rotor, $12{,}000 \times g$, 20 min, 4°C) and filter the supernatant fluid (0.45 μm pore size).
6. Prepare an AG1-8X column (2.3 × 30 cm) in formate form. Connect to an Äkta FPLC system.
7. Load the filtrate on the AG1-8X column, wash with 300 mL of deionized water, and elute with a gradient of 0–4.0 *M* ammonium formate in 0.1 *M* formic acid at flow rate of 0.5 mL/min.
8. Submit fractions to ^{31}P NMR. Use capillaries containing 17 m*M* phosphoric acid as external standard in each spectrum-recording.
9. Pool appropriate fractions and remove solvent by freeze-drying.

3.1.3.4 Notes

The results of an elution profile of the used growth medium of a *phnP* strain grown in the presence of **2** are shown in Fig. 4. Several compounds were detected: α-D-ribosyl-1′-(2-*N*-acetamidoethylphosphonate), 5′-phospho-α-D-ribosyl-1′-(2-*N*-acetamidoethylphosphonate), 2-*N*-acetamidoethylphosphonate, **11**, and Pi. By analogy, the culture medium of cells grown on **1** should contain α-D-ribosyl-1-methylphosphonate, **10**, α-D-ribosyl-1,2-cyclic phosphate, **11**, Pi, and residual **1**. In addition to the compounds mentioned, α-D-ribosyl-1-ethylphosphonate has been previously isolated (Avila et al., 1991). The elution profile of Fig. 4 is relatively complicated. This is because the cells were grown in the presence of **2**. Aminoalkylphosphonates are *N*-acetylated in a reaction catalyzed by *phnO*-specified aminoalkylphosphonate *N*-acetyltransferase (Errey & Blanchard, 2006; Hove-Jensen et al., 2012, 2014). Alkylphosphonates are not acetylated and a peak represented by 2-*N*-acetamidoethylphosphonate (Fig. 4, *blue squares*) would be absent in cultures grown with **1**.

3.2 Phn(GHIJ)$_2$K and Phn(GHIJ)$_2$ Protein Complexes

Following the cloning and sequencing of the *E. coli* 14-cistron operon *phnCDEFGHIJKLMNOP* that specify enzymes and other proteins

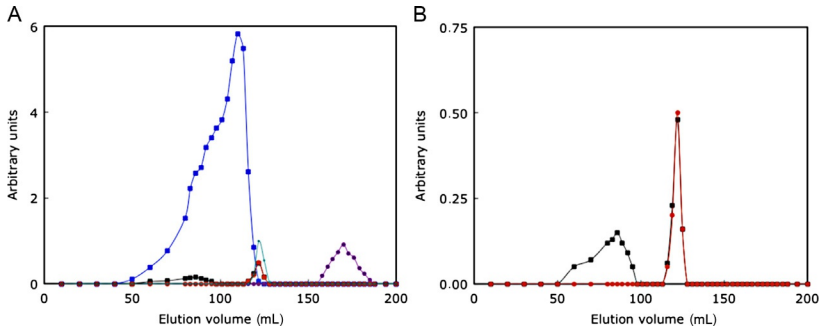

Fig. 4 Ion exchange chromatography of P-containing compounds synthesized by strain HO2542 (*ΔphnP ΔpstS*). Cells were grown at 37°C for 24 h in the presence of **2**. The used growth medium was applied to an AG1-8X column and after elution fractions were analyzed by ^{31}P NMR spectroscopy with 17 m*M* phosphoric acid as external standard (δ 0 ppm). *Black squares* represent chemical shift of δ 24 ppm, i.e., α-D-ribosyl-1′-(2-*N*-acetamidoethylphosphonate) (elution at 50–97 mL) and 5′-phospho-α-D-ribosyl-1′-(2-*N*-acetamidoethylphosphonate); *blue squares* represent δ 20 ppm, i.e., 2-*N*-acetamidoethylphosphonate; *purple circles* represent δ 18.6 ppm, i.e., α-D-ribosyl-1,2-cyclic phosphate; and *red circles* represent δ 3.6 ppm, i.e., P_i and 5′-phospho-α-D-ribosyl-1′-(2-*N*-acetamidoethylphosphonate). (A) Elution profile of all five compounds. (B) Blow-up of the elution profile of δ 24 ppm (*black squares*) and δ 3.6 ppm (*red circles*) (Hove-Jensen et al., 2012).

necessary for cleavage of C—P bonds by the C—P lyase pathway, it was suggested that PhnG, PhnH, PhnI, PhnJ, PhnK, PhnL, and PhnM constituted the C—P lyase (Chen et al., 1990). Later studies revealed that five of these polypeptides constitute a robust protein complex, the PhnGHIJK protein complex (Jochimsen et al., 2011). A variant of this protein complex, the PhnGHIJ protein complex, called the C—P lyase core complex, was subsequently crystallized, and its three-dimensional structure determined (Seweryn et al., 2015). Furthermore, PhnJ alone was able to cleave the C—P bond and as such constitutes the C—P lyase (Section 3.6) (Kamat, Williams, et al., 2011).

3.2.1 *Construction of Plasmid-Borne* phnGHIJK *and* phnGHIJ *Operons*

For maximal synthesis of *phn*-specified polypeptides, plasmids pHO571 and pHO572 containing the *phnGHIJK* and *phnGHIJ* cistrons, respectively, of the 14-cistron *E. coli phn* operon were constructed in the pUHE23-2 vector (H. Bujard, Heidelberg, personal communication), which carries a *bla* gene specifying ampicillin resistance. A variant of pHO571 (pHO575) containing a *phnK* allele specifying His_6-tagged versions of PhnK has also been constructed (Hove-Jensen et al., 2011). Cells harboring pUHE23-2-derived plasmid must be transformed in advance with a *lacI*^{q}-harboring episome such as

F *lacI*^{q} *zzf::*Tn*10* (which also specifies tetracycline resistance) to ensure repression of the cloned gene. Synthesis of the desired protein can then be achieved by induction of expression of the cloned gene by the addition of IPTG.

3.2.1.1 Equipment

- Microfuge with rotor for 1.5 mL tubes
- Thermocycler
- Incubators with thermostat and shaking device for growth of bacterial strains and enzyme incubation
- UV-spectrophotometer for measuring DNA concentrations
- Agarose gel electrophoresis apparatus

3.2.1.2 Materials and Reagents

- *E. coli* strain HO1429, a phosphonate growth proficient strain
- LB
- DNeasy Blood & Tissue Kit (Qiagen) for the isolation of *E. coli* chromosomal DNA
- QIAprep Spin Miniprep Kit (Qiagen) for the isolation of plasmid DNA
- QIAquick PCR Purification Kit (Qiagen) for the purification of PCR reactions
- The Long PCR Enzyme Mix PCR kit (Thermo Fisher Scientific) for amplification of large DNA fragments (>5 kbp)
- Restriction endonucleases EcoRI, HindIII, BstEII, BssHII, Mung Bean nuclease, and T4 DNA ligase
- Oligodeoxyribonucleotides 5′-AGAATTCATTAAAGAGGAGAAATTAACTATGCACGCAGATACCGCGACCC-3′ and 5′-GGAAGCTTGCATGCTTATTAGAACACCCTTTTACCCTGACGCC-3′ as primers (recognition sites for the restriction endonuclease *Eco*RI and *Hin*dIII are underlined)
- The four deoxyribonucleoside triphosphates
- DNA of pUHE23-2

3.2.1.3 Protocol

1. Chromosomal DNA is isolated from 1 mL of LB-grown HO1429 by the DNeasy procedure.
2. Mix on ice chromosomal DNA of HO1429, the four deoxyribonucleoside triphosphates, the oligodeoxyribonucleotides, buffer, and enzyme of the Long PCR Enzyme Mix. Adjust the PCR cycles according to the manufacturers' direction and run the PCR. Analyze the result by agarose gel electrophoresis.

3. The resulting 5660 bp PCR product is restricted by *Eco*RI and *Hind*III, and the liberated 5647-bp DNA fragment ligated to similarly restricted DNA of pUHE23-2 to generate pMN1 (*phnGHIJKLMN*).
4. The *phnL* and *phnM* cistrons are deleted from pMN1 by restriction with *Bst*EII and *Hind*III, followed by incubation with Mung Bean nuclease to create blunt ends, and then with T4 DNA ligase to create pHO571 (*phnGHIJK*).
5. The *phnK*, *phnL*, and *phnM* cistrons are removed from pMN1 DNA by partial *Bss*HII-restriction followed by *Hind*III, Mung Bean nuclease, and T4 DNA ligation to generate pHO572 (*phnGHIJ*).

3.2.2 Analytical Purification of Phn(GHIJ)$_2$K and Phn(GHIJ)$_2$ Protein Complexes

The expression of *phn* genes is induced in cells of strain HO2735 (*Δ(lac) Δ(phn)*/F (*lacI*^{q} *zzf::*Tn*10*)) (Hove-Jensen & Maigaard, 1993) carrying pHO571 or pHO572. The two protein complexes (PhnGHIJK and PhnGHIJ) are purified by the same procedure. The purification procedure is based on the small size of the PhnG polypeptide (16.5 kDa), which is located at the bottom of the gel after SDS-PAGE (i.e., in an area less populated with bands) and therefore relatively easy to identify (Fig. 5, lane 3).

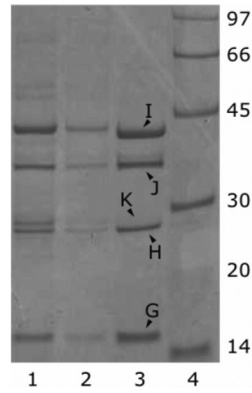

Fig. 5 Isolation of the PhnGHIJK protein complex from *phn*-haploid *E. coli* strain HO2568. The protein complex was purified by ion exchange in Q Sepharose. PhnG-containing fractions were mixed with the cobalt ion-containing resin, washed and submitted to SDS-PAGE. Lanes 1 and 2, two Q Sepharose fractions of cell extract after treatment with cobalt ion-containing resin; lane 3, purified PhnGHIJK protein complex; and lane 4, molecular mass standard. Values in kDa are given on the right-hand side.

Accordingly, after each purification step, fractions are analyzed by SDS-PAGE, and fractions appropriately enriched for PhnG are pooled and analyzed or further purified.

3.2.2.1 Equipment

- Incubator with thermostat and shaking device for growth of bacterial strains
- Sorvall centrifuge with SS-34 rotor
- Sonicator
- Q Sepharose Fast Flow column (1.6 × 7 cm) (GE Healthcare)
- Sephacryl S300 column (1.6 × 39 cm) (GE Healthcare)
- Äkta FPLC system (GE Healthcare)
- SDS-PAGE equipment

3.2.2.2 Materials and Reagents

- Strain HO2735 (*Δ(lac) Δ(phn)*/F (*lacI*^{q} *zzf::*Tn*10*) harboring pHO571 or pHO572
- NZY broth (Hove-Jensen and Maigaard, 1993) or LB
- Tetracycline and ampicillin at concentrations of 10 and 100 mg/L, respectively.
- IPTG, 50 m*M*
- Tris/HCl, 50 m*M*, pH 7.5
- Tris/HCl, 50 m*M*, pH 8.0, 1 m*M* EDTA
- Tris/HCl, 50 m*M*, pH 8.0, 150 m*M* NaCl
- Tris/HCl, 50 m*M*, pH 8.0, 1 m*M* EDTA, 10% (w/v) streptomycin sulfate
- Ammonium sulfate
- 1 *M* NaCl
- SDS-PAGE reagents

3.2.2.3 Protocol

A typical procedure for routine preparation of analytical amounts of protein complexes is as follows:

1. A culture (typically 50 mL) of the *phn* overexpressing strain is grown at 37°C to an OD_{600} of approximately 0.7 and cooled in ice for 30 min, at which time IPTG is added to a final concentration of 0.5 m*M*. Incubation is continued with shaking at 26–28°C for 3–4 h.

2. Cells are harvested by centrifugation, concentrated fourfold in 50 m*M* Tris/HCl pH 8.0, 1 m*M* EDTA, and broken by ultrasonic treatment while in ice and centrifuged to obtain a cleared lysate.
3. To 10 mL of a cleared lysate 1.2 mL of 10% (w/v) of streptomycin sulfate in 50 m*M* Tris/HCl pH 8.0, 1 m*M* EDTA, is added. The solution is stirred for 30 min, centrifuged in a Sorvall SS-34 rotor at 12,000 × *g* for 30 min.
4. The supernatant fluid is submitted to ion exchange by application to a Q Sepharose Fast Flow column (1.6 × 7 cm) connected to an Äkta FPLC system. The column had been previously equilibrated with 50 m*M* Tris/HCl, pH 7.5. After washing with 10 column volumes of the same buffer, protein is eluted with a linear gradient from 0 to 1 *M* sodium chloride over 10 column volumes at a flow rate of 1.2 mL/min. Fractions are analyzed by SDS-PAGE followed by staining in the presence of Coomassie Brilliant Blue R. Appropriate fractions are pooled, concentrated by ammonium sulfate precipitation, and redissolved in 0.5 mL of 50 m*M* Tris/HCl, pH 8.0, 150 m*M* sodium chloride.
5. The redissolved pellet is submitted to size exclusion chromatography by application to a Sephacryl S300 column (1.6 × 39 cm) equilibrated with 50 m*M* Tris/HCl, pH 8.0, 150 m*M* sodium chloride. Protein is eluted isocratically at a flow rate of 1 mL/min. Two milliliter fractions are collected and analyzed by SDS-PAGE. Appropriate fractions are pooled and concentrated or dialyzed.

3.2.3 Preparative Purification of the Phn(GHIJ)$_2$ Protein Complex

For crystallization of the PhnGHIJ protein complex, a different purification protocol is used. This procedure results in the isolation of larger quantities of pure PhnGHIJ protein complex (Jochimsen et al., 2011). Although none of the polypeptides of the Phn(GHIJ)$_2$ protein complex contain a His_6-tag, the protein complex binds tightly to Ni^{2+}-resins (Jochimsen et al., 2011). This effect is utilized during the purification protocol.

3.2.3.1 Equipment

- Incubator with thermostat and shaking device for growth of bacterial strains
- Culture flasks, 5 L
- Sorvall centrifuge equipped with SS-34 and GS3 rotors
- Emulsiflex C-5 high pressure homogenizer (Avestin Inc., Ottawa, Canada)
- Prepacked HisTrap HP column (5 mL) with Ni^{2+}-NTA agarose (GE Healthcare)

- Source 15Q anion exchange column (1 mL) (GE Healthcare)
- Superdex 200 10/300 GL size-exclusion column (GE Healthcare)
- Äkta FPLC system (GE Healthcare)
- SDS-PAGE equipment

3.2.3.2 Materials and Reagents

- Strain HO2735/pHO572
- LB
- IPTG, 0.05 *M*
- 50 m*M* HEPES, pH 7.5, 0.5 *M* NaCl, 5 m*M* $MgCl_2$, 20% (v/v) glycerol, 3 m*M* mercaptoethanol
- 50 m*M* HEPES, pH 7.5, 0.1 *M* NaCl, 5 m*M* $MgCl_2$, 5 m*M* mercaptoethanol
- 50 m*M* HEPES, pH 7.5, 0.3 *M* NaCl, 5 m*M* mercaptoethanol
- Complete Protease Inhibitor Cocktail (Sigma-Aldrich)
- NaCl, 1 *M*
- Imidazole, 4 *M*, pH 8.0

3.2.3.3 Protocol

1. Cells (strain HO2735/pHO572) are grown in 2 L of LB. At an OD_{600} of 0.8, gene expression is induced by the addition of IPTG to 0.5 m*M* and cells are incubated overnight at 18°C.
2. Cells are harvested by centrifugation (Sorvall GS3 rotor, 12,000 × *g*, 45 min, 4°C) and resuspended in 40 mL of 50 m*M* HEPES, pH 7.5, 0.5 *M* sodium chloride, 5 m*M* magnesium chloride, 20% (v/v) glycerol, 3 m*M* mercaptoethanol and half a tablet of Complete Protease Inhibitor Cocktail are added.
3. Cells are homogenized in an Emulsiflex C-5 at 15,000 p.s.i. followed by centrifugation (Sorvall SS-34 rotor, 12,000 × *g*, 45 min, 4°C) to generate a cleared lysate.
4. The cleared lysate (30 mL) is applied to Ni^{2+}-NTA agarose in a 5 mL prepacked HisTrap HP column and washed with 10 column volumes of 50 m*M* HEPES, pH 7.5, 0.3 *M* NaCl, 5 m*M* magnesium chloride, 20% (v/v) glycerol, 5 m*M* mercaptoethanol. The $Phn(GHIJ)_2$ protein complex is then eluted with 8 column volumes of the same buffer containing 0.25 *M* imidazole. The eluted complex is dialyzed overnight against 50 m*M* HEPES, pH 7.5, 0.1 *M* sodium chloride, 5 m*M* magnesium chloride, 5 m*M* mercaptoethanol at 4°C.
5. The dialyzed solution is applied to a 1 mL Source 15Q column preequilibrated with 50 m*M* HEPES, pH 7.5, 0.1 *M* sodium chloride,

5 m*M* magnesium chloride, 5 m*M* mercaptoethanol, and eluted with a linear gradient of 0.1–0.6 *M* sodium chloride over 10 column volumes.

6. Protein complex is finally purified on a Superdex 200 10/300 GL size-exclusion column equilibrated with 50 m*M* HEPES, pH 7.5, 0.3 *M* sodium chloride, 5 m*M* mercaptoethanol. The yield is typically 4–8 mg of pure PhnGHIJ protein complex.

3.2.4 Analytical Identification of PhnGHIJK Protein Complexes

The presence of the PhnGHIJK protein complex can be identified in haploid (i.e., plasmid-less) strains as long as these harbor a Pho regulon-constitutive mutation. One such strain is *E. coli* HO2568 (Δ*pstS*) (Hove-Jensen et al., 2012). Alternatively, cells may be grown under Pi limiting conditions (i.e., below 4 μ*M*) to induce expression of genes regulated by the external Pi supply (Hsieh & Wanner, 2010). The analytical procedure below is applicable to studies of protein–protein interactions of C − P lyase components of other organisms than *E. coli* as well.

The equipment, buffers, and reagents for analytical studies are identical to those described in Sections 3.2.2.1 and 3.2.2.2, with the exception of the use of a cobalt ion-containing resin such as Talon (Clontech Technologies, Inc.) to capture the PhnGHIJK protein complex. For unknown reasons the complex binds much more tightly to cobalt ion resins than nickel ion resins. Although denaturing conditions must be used to elute the PhnGHIJK polypeptides, the use of a cobalt ion resin is ideal for analytical detection of the complex.

3.2.4.1 Protocol

1. A culture (typically 50 mL) of the strain under analysis is incubated overnight (15–20 h) in LB medium at 37°C.
2. Cells are harvested by centrifugation (12,000 × *g*), resuspended in 12 mL of 50 m*M* Tris/HCl pH 8.0, 1 m*M* EDTA, and broken by ultrasonic treatment while in ice. The lysed cells are centrifuged in a Sorvall SS-34 rotor at 12,000 × *g* to obtain a cleared lysate.
3. To 10 mL of a cleared lysate 1.2 mL of 10% (w/v) of streptomycin sulfate in 50 m*M* Tris/HCl pH 8.0, 1 m*M* EDTA is added. The solution is stirred for 30 min then centrifuged in a Sorvall SS-34 rotor at 12,000 × *g* for 30 min.
4. The supernatant fluid is submitted to ion exchange by application to a Q Sepharose Fast Flow column connected to an Äkta FPLC platform and elution performed as described in step 4 of Section 3.2.2.3. Fractions

are analyzed by SDS-PAGE followed by staining in the presence of Coomassie Brilliant Blue R. Appropriate fractions are selected for further analysis.

5. A PhnG-containing fraction is mixed with an equal volume of the cobalt ion-resin and placed on ice and for 30 min with occasional shaking.
6. The resin is washed with buffer (50 m*M* Tris/HCl pH 8.0, 1 m*M* EDTA), centrifuged, the supernatant fluid removed, SDS-PAGE loading buffer (1 ×) added, and the sample is prepared for SDS-PAGE.

3.2.4.2 Notes

Occasionally a protein sample must be concentrated for analytical analyses. The protein sample is concentrated by mixing with one-fifth volume of 60% trichloroacetic acid, left in the cold overnight and centrifuged to recover the precipitate. A typical result is shown in Fig. 5. Two fractions (lanes 1 and 2) contain PhnG, PhnH, PhnK, PhnJ, and PhnI by comparison to purified PhnGHIJK protein complex (lane 3). It is therefore concluded that the PhnGHIJK protein complex is present in the haploid strain.

3.3 PhnI, Nucleosidase

3.3.1 Purification of PhnI

The *E. coli* gene *phnI* can be PCR amplified and cloned as a *N*-terminal GST fusion protein into a pET42a(+) vector as described previously (Kamat, Burgos, et al., 2013; Kamat, Williams, et al., 2011) with a Factor-Xa cleavage site between GST and PhnI.

3.3.1.1 Equipment

- Incubator with thermostat and shaking mechanism for growing of bacterial cultures
- Bacterial culture flasks, 3 L
- Centrifuge with adaptors and bottles for pelleting bacterial cells and lysates
- Prepacked GSTrap column (5 mL, GE Healthcare)
- Äkta FPLC system (GE Healthcare)
- SDS-PAGE equipment (Bio-Rad)

3.3.1.2 Materials and Reagents

- LB
- Kanamycin (50 mg/mL in sterile water)
- IPTG (0.5 *M* in sterile water)

- 100 m*M* HEPES at pH 8.8, 500 m*M* NaCl, 10% (v/v) glycerol, 1 m*M* dithiothreitol (DTT) and 1 m*M* EDTA
- Phenylmethylsulfonyl fluoride (PMSF) (Sigma-Aldrich)
- Protease Inhibitor Cocktail (PIC) (Sigma-Aldrich)
- DNAase I (Sigma-Aldrich)
- 100 m*M* HEPES at pH 8.8, 500 m*M* NaCl, 10% (v/v) glycerol, 1 m*M* DTT, 1 m*M* EDTA and 10 m*M* reduced glutathione

3.3.1.3 Protocol

1. The pET42a-*phnI* plasmid is transformed into *E. coli* BL21 (DE3) competent cells using standard protocols.
2. A single colony is inoculated and grown overnight at 37°C in 5 mL of LB medium containing 50 μg/mL kanamycin, and the 5 mL inoculum is used to inoculate 1 L of the same medium.
3. The 1 L cell culture is incubated at 37°C, till the OD_{600} reaches ~0.3, at which point the temperature is reduced to 15°C.
4. After approximately 1.5 h, when the OD_{600} is ~0.6, 0.5 m*M* IPTG is added to the 1 L culture to induce expression of the gene encoding the *N*-terminal GST fusion PhnI protein.
5. Approximately 24 h after IPTG addition, the cells are harvested by centrifugation at 12,000 × *g* for 15 min at 4°C and used immediately for purification of PhnI (Kamat, Burgos, et al., 2013).
6. The pelleted cells are resuspended in 100 m*M* HEPES at pH 8.8, containing 500 m*M* NaCl, 10% (v/v) glycerol, 1 m*M* dithiothreitol (DTT), and 1 m*M* EDTA (binding buffer), containing 0.1 mg/mL PMSF, 1 μL/mL of PIC, and 0.4 mg/mL DNAase I, and mixed to homogeneity by stirring in the binding buffer with additives at 4°C for 15 min.
7. Subsequently, the cells are lysed by sonication, and the soluble proteins are separated from the cellular debris by centrifugation at 12,000 × *g* for 10 min at 4°C. The resulting supernatant is applied to a GSTrap column (5 mL) previously equilibrated with 10 column volumes of the binding buffer.
8. The column is then washed with 10 column volumes of the binding buffer.
9. The protein is eluted with a linear gradient of reduced glutathione (0–10 m*M*) in 100 m*M* HEPES at pH 8.8, 500 m*M* NaCl, 10% (v/v) glycerol, 1 m*M* DTT, 1 m*M* EDTA over 15 column volumes at a flow rate of 5 mL/min.

10. The fractions are analyzed for purity by SDS-PAGE and appropriate fractions are pooled and concentrated using a 10,000 Da molecular weight cut off filter. Typical yields are 1 mg PhnI per liter culture (~4 g of cells/L of LB media).

3.3.1.4 Notes

1. Freeze thawing cells seemed to significantly reduce the yield and purity of PhnI.
2. The *N*-terminal GST fusion PhnI protein was found to precipitate at pH < 8.2; hence most PhnI assays were done in buffers with pH > 8.5. Additionally, for unknown reasons, DTT is critical for purifying active PhnI, i.e., freshly prepared DTT was used in all PhnI preparations and assays to avoid degradation in buffers over time.
3. PhnI is not stable and needs to be used immediately after eluting from the GST binding column, after assessing the purity of the fractions.

3.3.2 Assaying PhnI Nucleosidase Activity

The PhnI-GST fusion protein catalyzes the conversion of purine nucleoside triphosphates to form D-ribose-5-triphosphate and the corresponding free purine base. ATP and GTP are the best substrates for the nucleosidase activity of PhnI. For enzyme kinetic assays with ATP, *E. coli* adenine deaminase (Ade) (Kamat, Bagaria, et al., 2011; Kamat, Holmes-Hampton, et al., 2011; Kamat & Raushel, 2013a) is used as a coupling enzyme, while with GTP *E. coli* guanine deaminase (GuaD) (Hall et al., 2010) is used as coupling enzyme. Both Ade and GuaD are capable of deaminating the respective free purine base but not the corresponding purine nucleoside triphosphate.

3.3.2.1 Equipment

- 96-well UV plate reader (SpectraMax Plus 384 μ-plate reader, Molecular Devices).
- 96-well UV-compatible quartz plate

3.3.2.2 Materials and Reagents

- 50 m*M* HEPES pH 8.5, 1 m*M* $MgCl_2$
- ATP or GTP (1 *M* each)
- Coupling enzyme (Ade or GuaD, 100 μ*M* each)

3.3.2.3 Protocol

1. All PhnI assays are performed in 50 m*M* HEPES, pH 8.5, containing 1 m*M* $MgCl_2$ at 30°C. In the assay, ATP or GTP concentrations are

varied from 0 to 300 μ*M*, the coupling enzyme (Ade or GuaD) is used at 10 μ*M*, and the reaction is initiated by the addition of PhnI-GST fusion protein at 1 μ*M*.

2. The final assay volume is 250 μL, performed in a 96-well plate, and time points are measured in a UV–visible spectrometer capable of reading a 96-well plate at wavelengths between 240 and 280 nm.
3. For reactions with ATP, the rate of conversion of adenine (released from ATP by PhnI-GST protein) to hypoxanthine by the deaminating action of Ade is monitored at 260 nm (decrease in adenine concentration) and quantified using the differential extinction coefficient of 4100 M^{-1} cm^{-1} at 260 nm (Kamat & Raushel, 2013a; Kamat, Williams, et al., 2011).
4. For reactions with GTP, the rate of conversion of guanine (released from GTP by PhnI-GST protein) to xanthine by the deaminating action of GuaD is monitored at 253 nm (decrease in guanine concentration) and quantified using the differential extinction coefficient of 3920 M^{-1} - cm^{-1} at 253 nm (Hall et al., 2010).
5. Typically, the assay is run for 30 min.

3.4 PhnI (PhnG, PhnH, PhnL), Glycosyltransferase

PhnI is purified as discussed in the previous section.

3.4.1 Purification of PhnG

The *E. coli* gene *phnG* can be PCR amplified and cloned into a pET30a(+) vector encoding a *N*-terminal His_6-tag as described earlier, and the recombinant plasmid bearing *phnG* is transformed into *E. coli* BL21 (DE3) competent cells (Kamat, Williams, et al., 2011).

3.4.1.1 Equipment

- Incubator with thermostat and shaking mechanism for growing of bacterial cultures
- Bacterial culture flasks, 3 L
- Centrifuge with adaptors and bottles for pelleting bacterial cells and lysates
- Prepacked His-Trap column (5 mL, GE Healthcare)
- Äkta FPLC system (GE Healthcare)
- SDS-PAGE equipment (Bio-Rad)

3.4.1.2 Materials and Reagents

- LB
- Kanamycin (50 mg/mL in sterile water)

- IPTG (0.5 *M* in sterile water)
- PMSF (Sigma-Aldrich)
- DNAase I (Sigma-Aldrich)
- Protamine sulfate (Sigma-Aldrich)
- 50 m*M* HEPES, 150 m*M* NaCl at pH 8.5, 20 m*M* imidazole
- 50 m*M* HEPES, 150 m*M* NaCl at pH 8.5, 1 *M* imidazole
- 50 m*M* HEPES, 150 m*M* NaCl at pH 8.5

3.4.1.3 Protocol

1. A single colony is inoculated and grown overnight at 37°C in 5 mL of LB medium containing 50 μg/mL kanamycin. Subsequently, the 5 mL culture is used to inoculate 1 L of the same medium.
2. The 1 L cell culture is incubated at 37°C until the OD_{600} reaches ~0.35, at which point the temperature is reduced to 18°C. After approximately 1 h, when the OD_{600} reaches ~0.6, IPTG is added to a final concentration of 0.5 m*M* to induce expression of *phnG*.
3. Approximately 18 h after IPTG addition the cells are harvested by centrifugation at 12,000 × *g* for 15 min at 4°C.
4. The pelleted cells are resuspended in 50 m*M* HEPES, 150 m*M* NaCl at pH 8.5, 20 m*M* imidazole (binding buffer), containing 0.1 mg/mL PMSF and sonicated. Debris is removed by centrifugation at 12,000 × *g* for 15 min at 4°C.
5. Nucleic acids are precipitated by the drop-wise addition (1 mL/min) of 2% w/v protamine sulfate at 4°C then removed by centrifugation at 12,000 × *g* for 15 min at 4°C.
6. The resulting supernatant fluid is applied to a Ni-NTA column (5 mL) previously equilibrated with 10 column volumes of the binding buffer.
7. The column is washed with 10 column volumes of the binding buffer.
8. The protein is eluted with a linear gradient of imidazole (0.02 to 1 *M*) in 50 m*M* HEPES, 150 m*M* NaCl at pH 8.5 over 20 column volumes at a flow rate of 5 mL/min.
9. The fractions are analyzed for purity of PhnG by SDS-PAGE. The appropriate fractions are pooled and dialyzed at 4°C into 50 m*M* HEPES, 150 m*M* NaCl at pH 8.5. The protein is concentrated using a 10,000 Da molecular weight cut off filter.
10. Typical yields for PhnG obtained are 15 mg PhnG per liter culture (~4 g of cells/L culture). PhnG can be flash frozen in 0.5 mL aliquots at 2 mg/mL protein concentration then stored at −80°C.

3.4.1.4 Notes

1. PhnG was found to precipitate at pH values <8.2; hence pH 8.5 was used in purification and assaying PhnG.

3.4.2 Purification of PhnH

The *E. coli* gene *phnH* can be PCR amplified and cloned into a pET28b(+) vector encoding a *N*-terminal His_6-tag as described earlier (Adams et al., 2008; Kamat, Williams, et al., 2011).

3.4.2.1 Equipment

- Incubator with thermostat and shaking mechanism for growing of bacterial cultures
- Bacterial culture flasks, 3 L
- Centrifuge with adaptors and bottles for pelleting bacterial cells and lysates
- Prepacked His-Trap column (5 mL, GE Healthcare)
- Äkta FPLC system (GE Healthcare)
- SDS-PAGE equipment (Bio-Rad)

3.4.2.2 Materials and Reagents

- LB
- Kanamycin (50 mg/mL in sterile water)
- IPTG (0.5 *M* in sterile water)
- PMSF (Sigma-Aldrich)
- Protease Inhibitor Cocktail (Sigma-Aldrich)
- DNAase I (Sigma-Aldrich)
- Protamine sulfate (Sigma-Aldrich)
- Binding buffer: 50 m*M* HEPES pH 8.0, 20 m*M* imidazole
- Elution Buffer: 50 m*M* HEPES pH 8.0, 1 *M* imidazole
- 50 m*M* HEPES pH 8.0.

3.4.2.3 Protocol

1. The recombinant plasmid bearing *phnH* is transformed into *E. coli* BL21 (DE3) competent cells. A single colony is inoculated and grown overnight at 37°C in 5 mL of LB medium containing 50 μg/mL kanamycin.
2. The 5 mL overnight culture is used to inoculate 1 L of the same medium. The 1 L cell culture is incubated at 37°C till the OD_{600} reaches ~0.4, at which point the temperature is reduced to 18°C. After

approximately 45 min, when the OD_{600} reaches ~0.6, IPTG is added to a final concentration of 0.5 m*M* to induce expression of *phnH*.

3. Approximately 16 h after IPTG addition the cells are harvested by centrifugation at 12,000 × *g* for 15 min at 4°C.
4. The pelleted cells are resuspended in 50 m*M* HEPES pH 8.0, 20 m*M* imidazole (binding buffer), containing 0.1 mg/mL PMSF and sonicated. Debris is removed by centrifugation at 12,000 × *g* for 15 min at 4°C.
5. Nucleic acids are precipitated by the drop-wise addition (1 mL/min) of 2% w/v protamine sulfate at 4°C then removed by centrifugation at 12,000 × *g* for 15 min at 4°C.
6. The resulting supernatant solution is applied to a Ni-NTA column (5 mL) previously equilibrated with 10 column volumes of the binding buffer.
7. The column was washed with 10 column volumes of the binding buffer.
8. The protein is eluted with a linear gradient of imidazole (0.02–1 *M*) in 50 m*M* HEPES, pH 8.0, over 20 column volumes at a flow rate of 5 mL/min.
9. The fractions are analyzed for purity by SDS-PAGE. Appropriate fractions are pooled and dialyzed at 4°C into 50 m*M* HEPES pH 8.0.
10. The protein is concentrated using a 10,000 Da molecular weight cut off filter. Typical yields for PhnH are 150 mg per liter culture (~4 g of cells/L culture). PhnH can be flash frozen in 0.5 mL aliquots at 10 mg/mL protein concentration then stored at –80°C.

3.4.3 Purification of PhnL

The *E. coli* gene *phnL* can be PCR amplified and cloned as a *N*-terminal GST fusion protein into a pET42a(+) vector as described earlier with a Factor-Xa cleavage site between GST and PhnL (Kamat, Williams, et al., 2011).

3.4.3.1 Equipment

- Incubator with thermostat and shaking mechanism for growing of bacterial cultures
- Bacterial culture flasks, 3 L
- Centrifuge with adaptors and bottles for pelleting bacterial cells and lysates
- Prepacked GSTrap column (5 mL, GE Healthcare)
- Äkta FPLC system (GE Healthcare)
- SDS-PAGE equipment

3.4.3.2 Materials and Reagents

- LB
- Kanamycin (50 mg/mL in sterile water)
- IPTG (0.5 *M* in sterile water)
- PMSF (Sigma-Aldrich)
- Protease Inhibitor Cocktail (Sigma-Aldrich)
- DNAase I (Sigma-Aldrich)
- 100 m*M* HEPES, at pH 8.5, 500 m*M* NaCl, 10% (v/v) glycerol, 1 m*M* DTT
- 100 m*M* HEPES, at pH 8.5, 500 m*M* NaCl, 10% (v/v) glycerol, 1 m*M* DTT, 10 m*M* reduced glutathione

3.4.3.3 Protocol

1. The recombinant plasmid encoding *phnL* as a *N*-terminal GST fusion construct is transformed into *E. coli* BL21 (DE3) competent cells.
2. A single colony is inoculated and grown overnight at 37°C in 5 mL of LB containing 50 μg/mL kanamycin. The 5 mL culture is then used to inoculate 1 L of the same medium.
3. The 1 L cell culture is incubated at 37°C till the OD_{600} reaches ~0.4, at which point the temperature is reduced to 18°C. After approximately 45 min, when the OD_{600} reaches ~0.6, IPTG is added to the culture to a final concentration of 0.5 m*M* in order to induce expression of *N*-terminal GST fusion PhnL protein.
4. The cells are harvested by centrifugation at 12,000 × *g* for 15 min at 4°C, 18 h after IPTG induction.
5. The pelleted cells are subsequently resuspended in 100 m*M* HEPES, at pH 8.5, containing 500 m*M* NaCl, 10% (v/v) glycerol, and 1 m*M* DTT (binding buffer), containing 0.1 mg/mL PMSF and 0.4 mg/mL DNAase I, and mixed to homogeneity by stirring at 4°C for 15 min.
6. The cells are lysed by sonication, and the soluble proteins are separated from the cellular debris by centrifugation at 12,000 × *g* for 10 min at 4°C.
7. The resulting supernatant solution is applied to a GSTrap column (5 mL) previously equilibrated with 10 column volumes of the binding buffer.
8. The column is washed with 10 column volumes of the binding buffer.
9. The protein is eluted with a linear gradient of reduced glutathione (0 to 10 m*M*) in 100 m*M* HEPES, pH 8.5, 500 m*M* NaCl, 10% (v/v) glycerol, 1 m*M* DTT over 15 column volumes at a flow rate of 5 mL/min.

10. The fractions are analyzed for purity of the PhnL-GST fusion protein by SDS-PAGE analysis; the appropriate fractions are pooled and concentrated using a 10,000 Da molecular weight cut off filter.
11. Typical yields are 8 mg of *N*-terminal GST fusion PhnL protein per liter culture (~4 g of cells/liter culture). PhnL can be flash frozen in 50 μL aliquots at 5 mg/mL protein concentration then stored at –80°C.

3.4.3.4 Notes

1. The PhnL GST-fusion protein was found to precipitate at pH < 8.0; hence pH 8.5 was used in all assays.
2. The PhnL GST fusion protein is stable through only one freeze–thaw cycle; therefore it is advised to freeze small aliquots.

3.4.4 Assaying PhnI (PhnG, PhnH, PhnL) Glycosyltransferase Activity

The combination of PhnI with PhnG, PhnH, and PhnL catalyzes the conversion of purine nucleoside triphosphate in the presence of **1** to form **9** and the corresponding free purine base (Kamat, Burgos, et al., 2013; Kamat, Williams, et al., 2011). ATP and GTP are the best substrates for the glycosyltransferase activity of the combined PhnI, G, H, L polypeptides. The coupling enzymes, the assay logic (measuring the free base released from the purine nucleoside triphosphate), and extinction coefficient are the same as those described in the aforementioned PhnI assays (Section 3.3.2).

3.4.4.1 Equipment

- 96-well UV plate reader (SpectraMax Plus 384 μ-plate reader, Molecular Devices).
- 96-well UV-compatible quartz plate

3.4.4.2 Materials and Reagents

- 50 m*M* HEPES pH 8.5, 1 m*M* **1**, 2 m*M* $MgCl_2$
- ATP or GTP (1 *M* each)
- Coupling enzyme (ADE or GuaD, each 100 μ*M*)
- Factor-Xa (New England Biolabs)

3.4.4.3 Protocol

1. All PhnIGHL assays are performed in 50 m*M* HEPES pH 8.5, 1 m*M* **1**, 2 m*M* $MgCl_2$ at 30°C.
2. In the assay, ATP or GTP (concentrations are varied from 0 to 300 μ*M*), the coupling enzyme (Ade or GuaD are used at 10 μ*M*) and Factor-Xa (10 units) are incubated at 30°C for 30 min,

3. The reaction was initiated by the addition of the PhnIGHL polypeptides [PhnI-GST fusion protein (0.1 μ*M*), PhnL-GST fusion protein (0.2 μ*M*), PhnG (0.4 μ*M*), and PhnH (0.4 μ*M*)] preincubated at 30°C in the assay plate.
4. Similar to the PhnI-GST fusion protein assays, the final assay volume is 250 μL in a 96-well plate, and time points are measured in a UV–visible spectrometer capable of reading a 96-well plate at wavelengths between 240 and 280 nm.
5. Typically, this assay is run for 30 min.

3.4.4.4 Notes

1. The concentration of **1** is kept constant in this assay.
2. The optimal ratio of the different components of the complex is determined empirically.
3. At the end of the assay protein may precipitate due to cleavage of the GST-tag from PhnI and PhnL fusion proteins.

3.5 PhnM, Diphosphohydrolase

3.5.1 Purification of PhnM

The *E. coli* gene *phnM* can be PCR amplified and cloned into a pET30a(+) vector as described earlier, and the recombinant plasmid bearing *phnM* is transformed into *E. coli* BL21 (DE3) competent cells (Kamat, Williams, et al., 2011).

3.5.1.1 Equipment

- Incubator with thermostat and shaking mechanism for growing of bacterial cultures
- Bacterial culture flasks, 3 L
- Centrifuge with adaptors and bottles for pelleting bacterial cells and lysates
- High Load 26/60 Superdex 200 prep grade gel filtration column (GE Healthcare)
- ResourceQ column (6 mL, GE Healthcare)
- Äkta FPLC system (GE Healthcare)
- SDS-PAGE equipment

3.5.1.2 Materials

- LB
- Kanamycin (50 mg/mL in sterile water)
- IPTG (0.5 *M* in sterile water)

- PMSF (Sigma-Aldrich)
- Protamine sulfate (Sigma-Aldrich)
- 100 m*M* HEPES, 1 m*M* $ZnCl_2$, pH 8.8
- 50 m*M* HEPES, pH 8.8
- 50 m*M* HEPES, pH 8.8, 1 *M* NaCl

3.5.1.3 Protocol

1. A single colony is inoculated and grown overnight at 37°C in 5 mL of LB medium containing 50 μg/mL kanamycin. The 5 mL culture is then used to inoculate 1 L of the same medium.
2. The 1 L cell culture is grown at 37°C until the OD_{600} reached ~0.35, at which point the temperature is reduced to 18°C. After approximately 1 h, when the OD_{600} reaches ~0.6, $ZnCl_2$ (1 m*M* final) is added, along with IPTG (0.5 m*M* final) to induce expression of *phnM*.
3. The cells are incubated for 20 h at 18°C and harvested by centrifugation. PhnM synthesis is confirmed by SDS-PAGE analysis of whole cells.
4. The cells are resuspended in 100 m*M* HEPES, 1 m*M* $ZnCl_2$, pH 8.8 (purification buffer), containing 0.1 mg/mL PMSF and lysed by sonication. Debris is removed by centrifugation at 12,000 × *g* for 15 min at 4°C.
5. The nucleic acids are precipitated at 4°C by drop-wise addition (1 mL/min) of 2% w/v protamine sulfate, and subsequently removed by centrifugation at 12,000 × *g* for 15 min at 4°C.
6. After centrifugation, solid ammonium sulfate is added to 60% (w/v) of the supernatant fluid at 4°C, to precipitate PhnM.
7. The precipitated protein is collected by centrifugation (12,000 × *g* for 15 min at 4°C), dissolved in purification buffer, and applied to a High Load 26/60 Superdex 200 prep grade gel filtration column, which is previously equilibrated with 3 column volumes of purification buffer.
8. Fractions enriched for PhnM, assessed by SDS-PAGE, are pooled and loaded onto a ResourceQ column (6 mL) preequilibrated with 10 column volumes of 50 m*M* HEPES, pH 8.8.
9. The column is washed with 10 column volumes of 50 m*M* HEPES, pH 8.8.
10. PhnM is eluted with a linear gradient of NaCl (0–1 *M*) in 50 m*M* HEPES, pH 8.8, over 20 column volumes.
11. Appropriate fractions, assessed by SDS-PAGE, are pooled and dialyzed into 100 m*M* HEPES, pH 8.8, 1 m*M* $ZnCl_2$.

12. Typical yields for PhnM are 4 mg/L culture (~4 g of cells/liter culture). PhnM can be flash frozen and stored at –80°C in 50 μL aliquots at a concentration of 5 mg/mL.

3.5.1.4 Notes

1. PhnM was found to precipitate at pH values <8.5; hence a pH of 8.8 was used for most PhnM assays.
2. The amount of ammonium sulfate required to precipitate PhnM is empirically determined, and may vary at times.
3. PhnM is stable for only 1 freeze–thaw cycle; therefore freezing small aliquots is advised.

3.5.2 Assaying PhnM Diphosphohydrolase Activity

The substrates for PhnM, **9** and **19** (Scheme 5), are synthesized as described earlier (Kamat, Williams, et al., 2011). PhnM assays are performed using a Pi Colorlock (Gold) phosphate detection colorimetric system (Innova Biosciences) according to the manufacturer's instructions. PhnM is a member of the amidohydrolase superfamily (Seibert & Raushel, 2005) and cleaves the phosphoanhydride bond of the α- and β-phosphoryl groups of the triphosphate moiety of **9** and **19,** releasing diphosphate; hence the phosphate detection kit is supplemented with commercially available inorganic diphosphatase to convert the released diphosphate to Pi that can be detected by the kit.

3.5.2.1 Equipment

- 96-well UV–visible plate reader (SpectraMax Plus 384 μ-plate reader, Molecular Devices)
- 96-well assay plate

3.5.2.2 Materials and Reagents

- Pi Colorlock (Gold) phosphate detection colorimetric system (Innova Biosciences)
- 50 m*M* HEPES, pH 8.8, 5 m*M* $MgCl_2$, 1 m*M* $ZnCl_2$
- Inorganic diphosphatase from Baker's yeast (Sigma-Aldrich)
- Compounds **9** or **19** (5 mM each)

3.5.2.3 Protocol

1. PhnM reactions are performed in 50 m*M* HEPES, pH 8.8, 5 m*M* $MgCl_2$, 1 m*M* $ZnCl_2$ with 5 U of inorganic diphosphatase from Baker's yeast.

2. As per manufacturer's instructions, a standard calibration curve is generated to establish the concentration of phosphate generated, and background phosphate if any is subtracted from each reading.
3. For PhnM kinetic analysis with **9** or **19**, a concentration range of 0–750 μ*M* of substrate is used, and the PhnM concentration is 10 n*M*.
4. In assays with either **9** or **19**, samples are collected at 0, 3, 6, 9, and 12 min. Each concentration and time point typically consists of three-independent replicates.
5. A plot of reaction rate vs substrate concentration is fitted to the Michaelis–Menten equation.

3.6 PhnJ, Carbon–Phosphorus Lyase

3.6.1 Purification and Anaerobic Reconstitution of PhnJ

The *E. coli* gene *phnJ* can be PCR amplified and cloned as a *N*-terminal GST fusion protein in the pET42a(+) vector as described earlier with a Factor-Xa cleavage site between PhnJ and GST (Kamat & Raushel, 2015; Kamat, Williams, et al., 2013, 2011).

3.6.1.1 Equipment

- Incubator with thermostat and shaking mechanism for growing of bacterial cultures
- Bacterial culture flasks, 3 L
- Centrifuge with adaptors and bottles for pelleting bacterial cells and lysates
- Anaerobic chamber (MBraun LabMaster SP glovebox).
- Äkta FPLC system (GE Healthcare)
- GSTrap column (GE Healthcare, 5 mL)
- SDS-PAGE equipment

3.6.1.2 Materials and Reagents

- LB
- Kanamycin (50 mg/mL in sterile water)
- IPTG (0.5 *M* in sterile water)
- PMSF (Sigma-Aldrich)
- Protease Inhibitor Cocktail (PIC) (Sigma-Aldrich)
- DNAase I (Sigma-Aldrich)
- Ferrous ammonium sulfate hexahydrate (Sigma-Aldrich)
- L-cysteine (Sigma-Aldrich)

- 150 m*M* HEPES, 500 m*M* NaCl, 10% (w/v) glycerol, 100 μ*M* dithionite and 50 μ*M* DTT, pH 8.5.
- 150 m*M* HEPES, 500 m*M* NaCl, 10% (w/v) glycerol, 100 μ*M* dithionite, 50 μ*M* DTT, 10 m*M* reduced glutathione, pH 8.5.

3.6.1.3 Protocol

1. The recombinant plasmid encoding *phnJ* as a *N*-terminal GST fusion gene construct is transformed into *E. coli* BL21 (DE3) competent cells.
2. A single colony is grown for 12 h at 37°C in 10 mL of LB containing 50 μg/mL kanamycin. The 10 mL inoculum is added to a 1.5 L culture of the same media.
3. The 1.5 L cell culture is grown at 37°C with a shaking at 200 r.p.m. till the OD_{600} reaches ~0.45, at which point the culture is cooled to 4°C in a cold room without shaking for 45 min (to prevent aeration prior to formation of the iron sulfur cluster).
4. Post cooling, 200 mg of solid ferrous ammonium sulfate hexahydrate (35 μ*M* final concentration) and 200 mg of solid L-cysteine (1.1 m*M* final concentration) is added, and the culture is allowed to stand for an additional 15 min at 4°C with no shaking.
5. The culture is subsequently transferred to a shaker precooled to 15°C with a shaking speed of 50 r.p.m. After incubation for 10 min, 75 μ*M* IPTG (final concentration) is added to induce *phnJ* expression.
6. The culture is allowed to incubate at 50 r.p.m. at 15°C for 24 h after IPTG addition. Expression of *phnJ* is confirmed by SDS-PAGE analysis.
7. The cells are harvested by centrifugation at 12,000 × *g* for 15 min.
8. This growth and expression method typically affords 1 g cells/L of culture.
9. All subsequent purifications of PhnJ (wild type and mutants) are performed in an anaerobic chamber cooled to 10°C, with the oxygen levels <4 ppm.
10. All buffers are degassed prior to introduction into the anaerobic chamber. The reductants, dithionite and DTT, are introduced as solids into the anaerobic chamber and added to buffers.
11. The cells are introduced into the anaerobic chamber precooled to 10°C, and resuspended in 150 m*M* HEPES, 500 m*M* NaCl, 10% (w/v) glycerol, 100 μ*M* dithionite, and 50 μ*M* DTT, pH 8.5 (binding buffer) containing 1 μL/mL PIC, 0.2 mg/mL PMSF, and 1 mg/mL DNAase I. The cells are mixed to homogeneity by stirring for 15 min.

12. The cells are lysed by sonication, and debris is removed by centrifugation at 12,000 × *g* for 10 min at 4°C under anaerobic conditions.
13. After centrifugation, the supernatant is applied to a GSTrap column (5 mL) previously equilibrated with 10 column volumes of the binding buffer.
14. The column is washed with 10 column volumes of the binding buffer.
15. The protein is eluted with a linear gradient of glutathione (0–10 m*M*) in 150 m*M* HEPES, 500 m*M* NaCl, 10% (w/v) glycerol, 100 μ*M* dithionite, 50 μ*M* DTT, pH 8.5, over 20 column volumes at a flow rate of 5 mL/min.
16. The protein eluting from the column is brown in color (due to the presence of an oxidized iron sulfur cluster), and fractions containing PhnJ-GST fusion protein are identified visually and purity is assessed by SDS-PAGE.
17. Appropriate fractions are pooled, and concentrated using a 10,000 Da molecular weight cut off filter.
18. The purification scheme typically affords 1 mg/L of culture of PhnJ-GST fusion protein.

3.6.1.4 Notes

1. The 50 r.p.m. shaking speed is set empirically and may vary. This is the minimum speed needed to suspend the cells and minimize aeration in order to allow maturation of the iron sulfur cluster within PhnJ.

3.6.2 Assaying PhnJ C—P Bond Cleaving Activity

PhnJ is a member of the radical SAM superfamily (Broderick et al., 2014), and cleaves the C—P bond of **10** to form **11** and methane (Scheme 1) (Kamat & Raushel, 2015). PhnJ reactions are performed in an anaerobic chamber with oxygen levels <4 ppm using freshly prepared enzyme (Kamat, Williams, et al., 2013, 2011). The PhnJ reaction product **10** can be purified from the reaction solution by a sequence of centrifugation and ultrafiltration to remove proteins followed by anion exchange chromatography as described previously (Kamat, Williams, et al., 2011) and in Section 3.1.3.

3.6.2.1 Equipment

1. Anaerobic chamber (MBraun LabMaster SP glovebox).
2. LC–MS (ESI-QTOF)
3. C18 HPLC column with 3 μm particle size, 15 cm length, and 3 mm internal diameter.

4. All ^{1}H and ^{13}C NMR experiments are performed on a Bruker Avance III 500 MHz NMR spectrometer equipped with a HCN cryoprobe.
5. The ^{31}P NMR (D_2O, 85% H_3PO_4 corresponds to $\delta = 0.00$) samples are analyzed using a Bruker Avance III 400 MHz NMR spectrometer or a Varian Unity Inova 500 MHz NMR spectrometer.
6. Airtight GC compatible vial (1.5 mL) with a screw cap fitted with a self-sealing rubber septum.

3.6.2.2 Materials and Reagents

1. 150 m*M* HEPES, 500 m*M* NaCl, 10% (w/v) glycerol, pH 8.5
2. Factor-Xa (New England Biolabs)
3. 5 m*M* ammonium acetate, pH 6.6
4. 75% (v/v) methanol in deionized distilled water

3.6.2.3 Protocol for the PhnJ Reaction

1. A typical PhnJ reaction contains: 120–140 μ*M* PhnJ-GST fusion protein, 2 m*M* SAM, 1 m*M* sodium dithionite, 1× Factor-Xa buffer (New England Biolabs) in 150 m*M* HEPES, 500 m*M* NaCl, 10% (w/v) glycerol, pH 8.5 in a reaction volume of 200 μL.
2. Depending on the experiment, different amounts of **10** are added to the reaction solution described in step 1. For single turnover experiments, 60 μ*M* **10** (0.5 PhnJ-GST fusion protein equivalent) is used. For multiple turnover experiments, 3 m*M* **10** (10–15 PhnJ-GST fusion protein equivalents) is used.
3. The reaction is initiated by addition of 50 U of Factor-Xa (New England Biolabs) for the *in situ* cleavage of the *N*-terminal GST tag, and the reactions are allowed to proceed for 8 h.
4. The reaction mixtures are centrifuged at 12,000 × *g* to separate precipitated PhnJ and/or GST and/or PhnJ-GST fusion protein.
5. Soluble proteins, if any, are removed using a 3000 Da molecular weight cut off filter by centrifugation.
6. The flow-through (~150 μL) is analyzed for the desired products.

3.6.2.4 Protocol for LC–MS/MS Analysis of PhnJ Reaction Products

1. For the detection, characterization, and quantitation of 5′-deoxyadenosine **24** from SAM (Scheme 6), LC–MS/MS is used.
2. A fraction of the flow-through from the PhnJ reaction (20 μL) is run through a standard C18 HPLC column with 3 μm particle size, 15 cm length, and 3 mm internal diameter to purify **24** and the mass is

determined using an electrospray ionization source quadrupole time of flight (ESI-QTOF) mass spectrometer.

3. The buffer system used for the HPLC separation of **24** is 5 m*M* ammonium acetate, pH 6.6 (buffer A) and 75% (v/v) methanol in deionized distilled water (buffer B).
4. A typical LC-run consists of 55 min, with the following solvent run sequence post injection: 0.3 mL/min 0% buffer B for 5 min, 0.5 mL/min 0% buffer B for 5 min, 0.5 mL/min linear gradient of buffer B from 0% to 100% over 25 min, 0.5 mL/min of 100% buffer B for 10 min, and reequilibration with 0.5 mL/min of 0% buffer B for 10 min.

3.6.2.5 Protocol for GC Detection of Methane Production by PhnJ

1. The reactions for the detection and analysis of methane are performed in an airtight vial (1.5 mL) with a screw cap fitted with a self-sealing rubber septum to allow injection.
2. For these reactions, all the aforementioned ingredients except for Factor-Xa are incubated in the vial and the contents made airtight.
3. The reaction is initiated by the injection of 50 U of Factor-Xa using an insulin syringe.
4. The headspace is analyzed for methane using gas chromatography (GC) and methane-labeling experiments are performed using gas chromatography with tandem mass spectrometry (GC–MS).
5. The GC and GC–MS instrumentation and experimental parameters are as described earlier (Kamat, Williams, et al., 2013).

3.6.2.6 Notes

Freeze thawing of the PhnJ-GST fusion protein yields inactive and often precipitated protein.

3.7 PhnP, 5-Phospho-α-D-Ribosyl 1,2-Cyclic Phosphodiesterase

The activity of C—P lyase (i.e., PhnJ) results in the formation of **11** (Scheme 1). In the remaining steps of the C—P lyase pathway, the cyclic phosphate is hydrolyzed to obtain **12** in a reaction catalyzed by *phnP*-specified phosphoribosyl cyclic phosphodiesterase. Although **11** is the native substrate for PhnP, the enzyme also hydrolyzes α-D-ribosyl-1,2-cyclic phosphate, i.e., a dephosphorylated derivative of **11** (Hove-Jensen et al., 2011). Both of these compounds can be isolated from the culture medium of an *E. coli ΔphnP* strain grown in the presence of a Pn (e.g., **1** or **2**) as described in Section 3.1.3. The phosphodiesterase also hydrolyzes cyclic

nucleotides such as 2′,3′-cyclic adenosine 5′-monophosphate, 2′,3′-cyclic guanosine 5′-monophosphate, and 2′,3′-cyclic cytidine 5′-monophosphate (Podzelinska et al., 2009), as well as a large number of synthetic phosphate diesters such as substituted methyl phenylphosphodiesters (He et al., 2011).

3.7.1 Purification of Phosphoribosyl Cyclic Phosphodiesterase PhnP

The purification protocol for PhnP is based on overexpression of an *E. coli phnP* gene specifying a His_6 tagged variant of the wild-type enzyme and affinity chromatography on nickel ion-containing agarose (Podzelinska et al., 2008).

3.7.1.1 Equipment

- Sterilization facilities
- Incubator with thermostat and shaking device
- Sterile 5 L flasks
- Spectrophotometer for optical density (OD) measurement at 600 nm. An OD of 1 (1 cm-light path) corresponds to approximately 6×10^{11} cells per L
- Centrifuge for 50 mL tubes and for 250 or 500 mL flasks
- Emulsiflex-C5 homogenizer (Avestin, Ottawa, Canada)
- Äkta FPLC system (GE Healthcare)
- SDS-PAGE apparatus
- Superdex 200 column prep-grade (1×30 cm) (GE Healthcare)
- Ultra centrifugal filters (10 kDa molecular weight cut off) (Amicon)
- Syringe for ultrafiltration
- 0.22 μm filters (Amicon)
- Nickel-nitrilotriacetic acid (Ni-NTA) agarose column (Qiagen)

3.7.1.2 Materials and Reagents

- Strain BL21 (DE3) containing p*LacI* (Novagen) and pHO520 (*phnP*)
- IPTG, 50 m*M*
- LB
- Ampicillin (10 g/L)
- Chloramphenicol (3 g/L)
- 50 m*M* phosphate buffer, pH 7.2, 10 m*M* imidazole, 0.3 *M* sodium chloride
- 50 m*M* phosphate buffer, pH 7.2, 0.5 *M* imidazole, 0.3 *M* sodium chloride
- 50 m*M* HEPES pH 7.2, 0.15 *M* sodium chloride

The purification protocol described below is based on the procedure described previously (Podzelinska et al., 2008).

3.7.1.3 Protocol

1. Inoculate aseptically strain BL21 (DE3) p*LacI* pHO520 in 50 mL of LB containing ampicillin (100 mg/L) and chloramphenicol (30 mg/L) in a 0.5 L flask. Incubate overnight at 30°C with aeration by shaking.
2. Transfer the overnight culture aseptically to a sterile 5 L flask containing 2 L of LB supplemented with ampicillin (100 mg/L) and chloramphenicol (30 mg/L) prewarmed at 30°C. Incubate at 30°C with aeration by shaking and follow OD_{600}.
3. At an OD_{600} of 0.6, add 20 mL of 50 m*M* IPTG to the culture and continue incubation at 15°C for 20 h.
4. Harvest the cells by centrifugation at $3000 \times g$ for 20 min at 4°C. Discard the supernatant fluid and resuspend the cells in 40 mL of 50 m*M* phosphate buffer, pH 7.2, 10 m*M* imidazole, 0.3 *M* sodium chloride.
5. Homogenize the cells by passage through an Emulsiflex-C5 homogenizer and remove debris by centrifugation at $40{,}000 \times g$ for 30 min at 4°C.
6. Load the supernatant to an Ni-NTA agarose column connected to an ÄKTA FPLC system and elute PhnP with a linear gradient of 10 m*M* to 0.5 *M* imidazole in 50 m*M* phosphate buffer, pH 7.2, 0.3 *M* sodium chloride over 15 column volumes at a flow rate of 5 mL/min.
7. Submit fractions to SDS-PAGE, pool appropriate fractions, and concentrate the protein solution to 1 mL.
8. Load the sample to a Superdex 200 column (1×30 cm) preequilibrated with 50 m*M* HEPES pH 7.2, 0.15 *M* sodium chloride, and elute isocratically at 2 mL/min. After analysis of fractions by SDS-PAGE, appropriate fractions are pooled and concentrated by passage through an ultrafiltration filter followed by passage through a 0.22 μm filter.
9. Flash freeze 200 μL aliquots of PhnP in liquid nitrogen and freeze at −80°C.

3.7.2 Assay of PhnP Activity

The hydrolytic activity of PhnP can be readily measured using synthetic arylphosphate diesters, such as *bis*(*p*-nitrophenyl)phosphate (bpNPP). Because PhnP does not have monoesterase activity, the rate of phenolate production reflects hydrolysis of one of the diester bonds. Moreover, by using methyl(phenyl)phosphates as substrates, the better aryl leaving groups

can be modified with substituents to modulate the pK_a of the conjugate acid of the leaving group. By measuring kinetic parameters for a series of substituted methyl(phenyl)phosphates one can perform a Brönsted analysis (He et al., 2011). This can provide information on the degree of charge stabilization that is occurring on the leaving group and phosphoryl oxygens in the transition state.

3.7.2.1 Equipment

- Spectrophotometer with temperature controlled cuvette holder for measurement of absorbance at 400 nm (e.g., Cary 300 Bio by Varian)
- Semimicro plastic cuvettes (e.g., BrandTech™, #759086D)
- Parafilm
- Gilson pipette set (P1000, P200, P20), used for pipetting reaction buffer.
- Hamilton syringes (10 μL, 25 μL, 100 μL), used for adding PhnP and substrate to the reaction. Reserve separate syringes for PhnP and substrate solutions.

3.7.2.2 Materials and Reagents

- Reaction buffer: 50 mL of 50 m*M* Tris/HCl, 150 m*M* NaCl, pH 7.1 in a 50 mL Falcon tube. Keep at room temperature.
- 1 mL of 50 m*M* $MnCl_2$ in reaction buffer.
- 1 mL of 100 mg/mL BSA (Sigma-Aldrich, 05479) in reaction buffer. Store on ice during assay.
- 20 mM bpNPP in reaction buffer. The extinction coefficient for *p*-nitrophenolate at pH 7.1 is $\varepsilon_{405} = 11{,}500\, M^{-1}\, cm^{-1}$. Store on ice during assay.
- PhnP stock solution. The concentration of PhnP is determined by using the extinction coefficient $\varepsilon_{280} = 33{,}835\, M^{-1}\, cm^{-1}$ which is calculated from the amino acid sequence using the ProtParam web tool (https://web.expasy.org/cgi-bin/protparam/protparam) (Gasteiger et al., 2005; Podzelinska et al., 2008). Typically, one requires 100–200 μL of 200 μ*M* PhnP in reaction buffer to acquire sufficient data points for a Michaelis–Menten plot. The stock solution is stored on ice during the assay.

3.7.2.3 Protocol

1. Set the cuvette holder temperature of the spectrometer to 25°C.
2. Prepare stock solutions of PhnP (200 μ*M*) and bpNPP (20 m*M*) in reaction buffer in 1.5 mL Eppendorf tubes. The PhnP solution must be freshly prepared from a −80°C freezer stock or newly purified enzyme.

Solutions of bpNPP can be stored at −20°C. During assays, the PhnP and bpNPP solutions should be kept on ice.

3. Add 650 μL of reaction buffer and 8 μL of 100 mg/mL BSA to a semi-micro cuvette using P1000 and P10 Gilson pipettes. The volume of reaction buffer can be altered to accommodate differing volumes of bpNPP solution. The final reaction volume is 750 μL.
4. Add 15 μL of 50 m*M* $MnCl_2$ in reaction buffer using a P20 Gilson pipette.
5. Add 10–200 μL of bpNPP solution using an appropriate Hamilton syringe.
6. Seal the top of the cuvette with three layers of Parafilm. Mix the reaction solution gently with inversion.
7. Place in the cuvette holder of the spectrometer and preincubate at 25°C for 10 min.
8. Measure 10–20 μL of PhnP solution using an appropriate Hamilton syringe.
9. Remove the preequilibrated cuvette and inject the PhnP solution directly into the reaction solution by puncturing the Parafilm. Gently invert the cuvette 3× to mix, wipe the exterior with a Kimwipe, and then return the vessel to the cuvette holder.
10. Monitor the increase in absorbance at 400 nm for 5–10 min. Derive an initial rate (V_o) from a linear region of this plot. An ideal rate of production of *p*-nitrophenolate is $dA400/dt = 0.05–0.2\,min^{-1}$. If the rate is too slow, or too fast, simply adjust the volume of PhnP.
11. Repeat the experiment using bpNPP concentrations ranging from 0.2× to 5× the final determined K_M value.
12. Kinetic parameters can be derived from a fit of V_o on bpNPP concentration with the Michaelis–Menten equation using GraFit or SigmaPlot. Under these assay conditions using bpNPP as the substrate, PhnP has kinetic parameters of $k_{cat} = 1.19 \pm 0.08\,s^{-1}$, $K_M = 2.9 \pm 0.5$ m*M*, and $k_{cat}/K_M = 410\,s^{-1}\,M^{-1}$ (Podzelinska et al., 2009).

3.7.2.4 Notes

1. A standard PhnP reaction is performed at 25°C in 50 m*M* Tris–HCl and 150 m*M* NaCl (pH 7.1), containing 1 mg/mL bovine serum albumin (BSA) and 1.0 m*M* $MnCl_2$. The BSA is added to prevent nonspecific binding of PhnP to the walls of the cuvette (this is a general strategy when assaying an enzyme at high dilution).
2. PhnP is most active in the presence of Mn^{2+}, and copurifies with this metal ion, but is equally active with Ni^{2+} (Podzelinska et al., 2009).

PhnP also copurifies with a tightly bound, structural Zn^{2+} ion. PhnP cannot be purified from *E. coli* in a fully metal ion-loaded form (only 0.1 manganese ion per active site) and displays saturation kinetics with respect to manganese ion concentration with an apparent K_M value of 130 μ*M*. Therefore, a concentration of 1 m*M* $MnCl_2$ in the reaction ensures the PhnP active site is saturated with metal ion.

3. The PhnP reaction is initiated by the addition of a concentrated aliquot (5–20 μL) of PhnP to the reaction solution using a 10 or 25 μL Hamilton syringe. The final concentration of PhnP can be adjusted from 0.5 to 20 μ*M*, depending on the reactivity of the substrate used, such that only 5%–15% of the substrate is consumed over 5–10 min.
4. The Hamilton syringe used to add PhnP or bpNPP solutions should be rinsed by pipetting and discarding a minimal volume of the stock solution (e.g., 10–20 μL), 3×, prior to adding the required volume to the reaction solution.
5. PhnP exhibits cooperative kinetics with bpNPP. However, this effect is weak, and therefore application of the standard Michaelis–Menten equation has a minimal impact on the calculated k_{cat} and K_M values.

4. SUMMARY

Given that life first evolved in the world's oceans, the cycle of biosynthesis and catabolism of **1** by MpnS and the C—P lyase pathway is likely an ancient one (McGrath et al., 2013). The utility of these enzymes is seen in their evolution and distribution. Although unique to marine microorganisms, the biosynthesis of **1** by MpnS arises from a catalytic scaffold that has been adapted to secondary metabolite biosynthesis by HEPD (phosphinothricin) and HppE (fosfomycin). An open question is why the biosynthesis of **1** by MpnS evolved in the first place. Is **1** a means of storing a Pi source for consumption during times of Pi depletion? Or a way of stabilizing biological structures (lipids, glycans, proteins) against phosphatases? An analysis of the distribution and structures of the biomolecules appended with **1** would be helpful in answering such questions. Locating such biomolecules will be facilitated by screening ocean microbial genomes for *mpnS* sequences.

Unlike MpnS, C—P lyase is not yet known to have formed a basis for any other chemistry other than catabolism of Pn and phosphite. This specialization is reflected by the unique sequences of many of the C—P lyase components, such as PhnG, PhnH, PhnI, and PhnJ, which do not align

with known protein or enzyme superfamilies, as well as the formation of a $Phn(GHIJ)_2K$ complex. The roles of the $Phn(GHIJ)_2K$ complex and several of the C—P lyase components (PhnG, H, K, L) to catalysis remains unknown. Although C—P lyase is dedicated to Pn catabolism, the system has a wide Pn substrate specificity, and thus offers much greater versatility than any other known Pn catabolic pathway. It is tempting to attribute complexity of the C—P lyase system, particularly the incorporation of **1** and other Pn into ribose prior to C—P bond cleavage, as the price for this versatility: by providing a common chemical handle (5-phospho-α-D-ribose), the transition state leading to C—P bond cleavage by PhnJ can be stabilized for a wide variety of Pn structures (and highly variable carbon radical stability). This versatility may also explain why C—P lyase is widely distributed in microbes, including terrestrial ones and those that live in Pi-rich environments (e.g., *E. coli*) (Villarreal-Chiu & Quinn, 2012). The distribution and persistence of the C—P lyase pathway thus underscore the biological necessity of Pi acquisition and the global distribution of Pn.

ACKNOWLEDGMENTS

We thank Bjarne Jochimsen, Aarhus University, for assistance with the analytical analysis of the PhnGHIJK protein complex. E.C.U. thanks the National Institutes of Health for funding (P01 GM077596 to Wilfred van der Donk). D.L.Z. thanks the Natural Sciences and Engineering Research Council (NSERC) of Canada for funding through the Discovery, Accelerator, and Strategic Grant programs. S.S.K. thanks IISER Pune for funding. We also thank Wilfred van der Donk, University of Illinois at Urbana-Champaign, for insightful comments.

REFERENCES

Adams, M. A., Luo, Y., Hove-Jensen, B., He, S. M., van Staalduinen, L. M., Zechel, D. L., et al. (2008). Crystal structure of PhnH: An essential component of carbon-phosphorus lyase in *Escherichia coli*. *Journal of Bacteriology*, *190*(3), 1072–1083. https://doi.org/10.1128/JB.01274-07.

Aono, R., Sato, T., Imanaka, T., & Atomi, H. (2015). A pentose bisphosphate pathway for nucleoside degradation in Archaea. *Nature Chemical Biology*, *11*(5), 355–360. https://doi.org/10.1038/nchembio.1786.

Artimo, P., Jonnalagedda, M., Arnold, K., Baratin, D., Csardi, G., de Castro, E., et al. (2012). ExPASy: SIB bioinformatics resource portal. *Nucleic Acids Research*, *40*, W597–603 [Web server issue]. https://doi.org/10.1093/nar/gks400.

Avila, L. Z., Draths, K. M., & Frost, J. W. (1991). Metabolites associated with organophosphonate C-P bond cleavage: Chemical synthesis and microbial degradation of [^{32}P]-ethylphosphonic acid. *Bioorganic & Medicinal Chemistry Letters*, *1*(1), 51–54. https://doi.org/10.1016/s0960-894x(01)81089-1.

Bernhard, S. A., & MacQuarrie, R. A. (1973). Half-site reactivity and the "induced-fit" hypothesis. *Journal of Molecular Biology*, *74*(1), 73–78.

Born, D. A., Ulrich, E. C., Ju, K.-S., Peck, S. C., van der Donk, W. A., & Drennan, C. L. (2017). Structural basis for methylphosphonate biosynthesis. *Science (New York, N.Y.)*, *358*(6368), 1336–1339. https://doi.org/10.1126/science.aao3435.

Bowman, E., McQueney, M., Barry, R. J., & Dunaway-Mariano, D. (1988). Catalysis and thermodynamics of the phosphoenolpyruvate/phosphonopyruvate rearrangement. Entry into the phosphonate class of naturally occurring organophosphorus compounds. *Journal of the American Chemical Society*, *110*(16), 5575–5576. https://doi.org/10.1021/ja00224a054.

Broderick, J. B., Duffus, B. R., Duschene, K. S., & Shepard, E. M. (2014). Radical *S*-adenosylmethionine enzymes. *Chemical Reviews*, *114*(8), 4229–4317. https://doi.org/10.1021/cr4004709.

Chang, W.-C., Dey, M., Liu, P., Mansoorabadi, S. O., Moon, S.-J., Zhao, Z. K., et al. (2013). Mechanistic studies of an unprecedented enzyme-catalysed 1,2-phosphono-migration reaction. *Nature*, *496*(7443), 114–118. https://doi.org/10.1038/nature11998.

Chang, W.-C., Mansoorabadi, S. O., & Liu, H.-W. (2013). Reaction of HppE with substrate analogues: Evidence for carbon-phosphorus bond cleavage by a carbocation rearrangement. *Journal of the American Chemical Society*, *135*(22), 8153–8156. https://doi.org/10.1021/ja403441x.

Chen, C. M., Ye, Q. Z., Zhu, Z. M., Wanner, B. L., & Walsh, C. T. (1990). Molecular biology of carbon-phosphorus bond cleavage. Cloning and sequencing of the *phn* (*psiD*) genes involved in alkylphosphonate uptake and C-P lyase activity in *Escherichia coli* B. *The Journal of Biological Chemistry*, *265*(8), 4461–4471.

Cicchillo, R. M., Zhang, H., Blodgett, J. A. V., Whitteck, J. T., Li, G., Nair, S. K., et al. (2009). An unusual carbon-carbon bond cleavage reaction during phosphinothricin biosynthesis. *Nature*, *459*(7248), 871–874. https://doi.org/10.1038/nature07972.

Cooke, H. A., Peck, S. C., Evans, B. S., & van der Donk, W. A. (2012). Mechanistic investigation of methylphosphonate synthase, a non-heme iron-dependent oxygenase. *Journal of the American Chemical Society*, *134*(38), 15660–15663. https://doi.org/10.1021/ja306777w.

DeLano, W. L. (2002). *The PyMOL molecular graphics system*. San Carlos, CA: DeLano Scientific.

Dyhrman, S. T., Benitez-Nelson, C. R., Orchard, E. D., Haley, S. T., & Pellechia, P. J. (2009). A microbial source of phosphonates in oligotrophic marine systems. *Nature Geoscience*, *2*(10), 696–699. https://doi.org/10.1038/ngeo639.

Dyhrman, S. T., Chappell, P. D., Haley, S. T., Moffett, J. W., Orchard, E. D., Waterbury, J. B., et al. (2006). Phosphonate utilization by the globally important marine diazotroph *Trichodesmium*. *Nature*, *439*(7072), 68–71. https://doi.org/10.1038/nature04203.

Errey, J. C., & Blanchard, J. S. (2006). Functional annotation and kinetic characterization of PhnO from *Salmonella enterica*. *Biochemistry*, *45*(9), 3033–3039. https://doi.org/10.1021/bi052297p.

Feingersch, R., Philosof, A., Mejuch, T., Glaser, F., Alalouf, O., Shoham, Y., et al. (2012). Potential for phosphite and phosphonate utilization by *Prochlorococcus*. *The ISME Journal*, *6*(4), 827–834. https://doi.org/10.1038/ismej.2011.149.

Frey, P. A., Hegeman, A. D., & Ruzicka, F. J. (2008). The radical SAM superfamily. *Critical Reviews in Biochemistry and Molecular Biology*, *43*(1), 63–88. https://doi.org/10.1080/10409230701829169.

Frost, J. W., Loo, S., Cordeiro, M. L., & Li, D. (1987). Radical-based dephosphorylation and organophosphonate biodegradation. *Journal of the American Chemical Society*, *109*(7), 2166–2171. https://doi.org/10.1021/ja00241a039.

Gardner, S. G., Johns, K. D., Tanner, R., & McCleary, W. R. (2014). The PhoU protein from *Escherichia coli* interacts with PhoR, PstB, and metals to form a phosphate-signaling complex at the membrane. *Journal of Bacteriology*, *196*(9), 1741–1752. https://doi.org/10.1128/JB.00029-14.

Gasteiger, E., Hoogland, C., Gattiker, A., Duvaud, S., Wilkins, M. R., Appel, R. D., et al. (2005). Protein identification and analysis tools on the ExPASy server. In *The proteomics protocols handbook,* (pp. 571–607): Humana Press. https://doi.org/10.1385/1-59259-890-0:571.

Gebhard, S., Busby, J. N., Fritz, G., Moreland, N. J., Cook, G. M., Lott, J. S., et al. (2014). Crystal structure of PhnF, a GntR-family transcriptional regulator of phosphate transport in *Mycobacterium smegmatis*. *Journal of Bacteriology*, *196*(19), 3472–3481. https://doi.org/10.1128/JB.01965-14.

Gebhard, S., & Cook, G. M. (2008). Differential regulation of high-affinity phosphate transport systems of *Mycobacterium smegmatis*: Identification of PhnF, a repressor of the *phnDCE* operon. *Journal of Bacteriology*, *190*(4), 1335–1343. https://doi.org/10.1128/JB.01764-07.

Gebhard, S., Tran, S. L., & Cook, G. M. (2006). The Phn system of *Mycobacterium smegmatis*: A second high-affinity ABC-transporter for phosphate. *Microbiology*, *152*, 3453–3465. https://doi.org/10.1099/mic.0.29201-0.

Ghodge, S. V., Cummings, J. A., Williams, H. J., & Raushel, F. M. (2013). Discovery of a cyclic phosphodiesterase that catalyzes the sequential hydrolysis of both ester bonds to phosphorus. *Journal of the American Chemical Society*, *135*(44), 16360–16363. https://doi.org/10.1021/ja409376k.

Hall, R. S., Fedorov, A. A., Marti-Arbona, R., Fedorov, E. V., Kolb, P., Sauder, J. M., et al. (2010). The hunt for 8-oxoguanine deaminase. *Journal of the American Chemical Society*, *132*(6), 1762–1763. https://doi.org/10.1021/ja909817d.

Hammerschmidt, F. (1991). Biosynthesis of natural products with a P–C bond. Part 8: On the origin of the oxirane oxygen atom of fosfomycin in *Streptomyces fradiae*. *Journal of the Chemical Society. Perkin Transactions 1*, 1993–1996. https://doi.org/10.1039/p19910001993.

Hammerschmidt, F., & Kaehlig, H. (1991). Biosynthesis of natural products with a phosphorus-carbon bond. 7. Synthesis of [1,1-^{2}H2]-, [2,2-^{2}H2]-, (*R*)- and (*S*)-[1-^{2}H1](2-hydroxyethyl)phosphonic acid and (*R*,*S*)-[1-^{2}H1](1,2-dihydroxyethyl)phosphonic acid and incorporation studies into fosfomycin in *Streptomyces fradiae*. *The Journal of Organic Chemistry*, *56*(7), 2364–2370. https://doi.org/10.1021/jo00007a022.

He, S.-M., Wathier, M., Podzelinska, K., Wong, M., McSorley, F. R., Asfaw, A., et al. (2011). Structure and mechanism of PhnP, a phosphodiesterase of the carbon-phosphorus lyase pathway. *Biochemistry*, *50*(40), 8603–8615. https://doi.org/10.1021/bi2005398.

Higgins, L. J., Yan, F., Liu, P., Liu, H.-W., & Drennan, C. L. (2005). Structural insight into antibiotic fosfomycin biosynthesis by a mononuclear iron enzyme. *Nature*, *437*(7060), 838–844. https://doi.org/10.1038/nature03924.

Hirao, H., & Morokuma, K. (2010). Ferric superoxide and ferric hydroxide are used in the catalytic mechanism of hydroxyethylphosphonate dioxygenase: A density functional theory investigation. *Journal of the American Chemical Society*, *132*(50), 17901–17909. https://doi.org/10.1021/ja108174d.

Hirao, H., & Morokuma, K. (2011). ONIOM(DFT:MM) study of 2-hydroxyethylphosphonate dioxygenase: What determines the destinies of different substrates? *Journal of the American Chemical Society*, *133*(37), 14550–14553. https://doi.org/10.1021/ja206222f.

Horsman, G. P., & Zechel, D. L. (2017). Phosphonate biochemistry. *Chemical Reviews*, *117*(8), 5704–5783. https://doi.org/10.1021/acs.chemrev.6b00536.

Hove-Jensen, B., Andersen, K. R., Kilstrup, M., Martinussen, J., Switzer, R. L., & Willemoës, M. (2017). Phosphoribosyl diphosphate (PRPP): Biosynthesis, enzymology, utilization, and metabolic significance. *Microbiology and Molecular Biology Reviews: MMBR*, *81*(1), e00040–16. https://doi.org/10.1128/MMBR.00040-16.

Hove-Jensen, B., & Maigaard, M. (1993). *Escherichia coli rpiA* gene encoding ribose phosphate isomerase A. *Journal of Bacteriology*, *175*(17), 5628–5635.

Hove-Jensen, B., McSorley, F. R., & Zechel, D. L. (2011). Physiological role of *phnP*-specified phosphoribosyl cyclic phosphodiesterase in catabolism of organophosphonic acids by the carbon-phosphorus lyase pathway. *Journal of the American Chemical Society*, *133*(10), 3617–3624. https://doi.org/10.1021/ja1102713.

Hove-Jensen, B., McSorley, F. R., & Zechel, D. L. (2012). Catabolism and detoxification of 1-aminoalkylphosphonic acids: *N*-acetylation by the *phnO* gene product. *PLoS One*, *7*(10), e46416. https://doi.org/10.1371/journal.pone.0046416.

Hove-Jensen, B., Rosenkrantz, T. J., Haldimann, A., & Wanner, B. L. (2003). *Escherichia coli phnN*, encoding ribose 1,5-bisphosphokinase activity (phosphoribosyl diphosphate forming): Dual role in phosphonate degradation and NAD biosynthesis pathways. *Journal of Bacteriology*, *185*(9), 2793–2801. https://doi.org/10.1128/JB.185.9.2793-2801.2003.

Hove-Jensen, B., Rosenkrantz, T. J., Zechel, D. L., & Willemoës, M. (2010). Accumulation of intermediates of the carbon-phosphorus lyase pathway for phosphonate degradation in *phn* mutants of *Escherichia coli*. *Journal of Bacteriology*, *192*(1), 370–374. https://doi.org/10.1128/JB.01131-09.

Hove-Jensen, B., Zechel, D. L., & Jochimsen, B. (2014). Utilization of glyphosate as phosphate source: Biochemistry and genetics of bacterial carbon-phosphorus lyase. *Microbiology and Molecular Biology Reviews: MMBR*, *78*(1), 176–197. https://doi.org/10.1128/MMBR.00040-13.

Hsieh, Y.-J., & Wanner, B. L. (2010). Global regulation by the seven-component Pi signaling system. *Current Opinion in Microbiology*, *13*(2), 198–203. https://doi.org/10.1016/j.mib.2010.01.014.

Huang, J., Su, Z., & Xu, Y. (2005). The evolution of microbial phosphonate degradative pathways. *Journal of Molecular Evolution*, *61*(5), 682–690. https://doi.org/10.1007/s00239-004-0349-4.

Jensen, K. F., Dandanell, G., Hove-Jensen, B., & Willemoes, M. (2008). Nucleotides, nucleosides, and nucleobases. *EcoSal Plus*, *3*(1). https://doi.org/10.1128/ecosalplus.3.6.2.

Jochimsen, B., Lolle, S., McSorley, F. R., Nabi, M., Stougaard, J., Zechel, D. L., et al. (2011). Five phosphonate operon gene products as components of a multi-subunit complex of the carbon-phosphorus lyase pathway. *Proceedings of the National Academy of Sciences of the United States of America*, *108*(28), 11393–11398. https://doi.org/10.1073/pnas.1104922108.

Ju, K.-S., Doroghazi, J. R., & Metcalf, W. W. (2014). Genomics-enabled discovery of phosphonate natural products and their biosynthetic pathways. *Journal of Industrial Microbiology & Biotechnology*, *41*(2), 345–356. https://doi.org/10.1007/s10295-013-1375-2.

Ju, K.-S., Gao, J., Doroghazi, J. R., Wang, K.-K. A., Thibodeaux, C. J., Li, S., et al. (2015). Discovery of phosphonic acid natural products by mining the genomes of 10,000 actinomycetes. *Proceedings of the National Academy of Sciences of the United States of America*, *112*(39), 12175–12180. https://doi.org/10.1073/pnas.1500873112.

Kamat, S. S., Bagaria, A., Kumaran, D., Holmes-Hampton, G. P., Fan, H., Sali, A., et al. (2011). Catalytic mechanism and three-dimensional structure of adenine deaminase. *Biochemistry*, *50*(11), 1917–1927. https://doi.org/10.1021/bi101788n.

Kamat, S. S., Burgos, E. S., & Raushel, F. M. (2013). Potent inhibition of the C-P lyase nucleosidase PhnI by Immucillin-A triphosphate. *Biochemistry*, *52*(42), 7366–7368. https://doi.org/10.1021/bi4013287.

Kamat, S. S., Holmes-Hampton, G. P., Bagaria, A., Kumaran, D., Tichy, S. E., Gheyi, T., et al. (2011). The catalase activity of diiron adenine deaminase. *Protein Science*, *20*(12), 2080–2094. https://doi.org/10.1002/pro.748.

Kamat, S. S., & Raushel, F. M. (2013a). Adenine deaminase. *Encyclopedia of Inorganic and Bioinorganic Chemistry*, 1–9.

Kamat, S. S., & Raushel, F. M. (2013b). The enzymatic conversion of phosphonates to phosphate by bacteria. *Current Opinion in Chemical Biology*, *17*(4), 589–596. https://doi.org/10.1016/j.cbpa.2013.06.006.

Kamat, S. S., & Raushel, F. M. (2015). PhnJ—A novel radical SAM enzyme from the C–P lyase complex. *Perspectives in Science*, *4*, 32–37. https://doi.org/10.1016/j.pisc.2014.12.006.

Kamat, S. S., Williams, H. J., Dangott, L. J., Chakrabarti, M., & Raushel, F. M. (2013). The catalytic mechanism for aerobic formation of methane by bacteria. *Nature*, *497*(7447), 132–136. https://doi.org/10.1038/nature12061.

Kamat, S. S., Williams, H. J., & Raushel, F. M. (2011). Intermediates in the transformation of phosphonates to phosphate by bacteria. *Nature*, *480*(7378), 570–573. https://doi.org/10.1038/nature10622.

Karl, D. M. (2014). Microbially mediated transformations of phosphorus in the sea: New views of an old cycle. *Annual Review of Marine Science*, *6*(1), 279–337. https://doi.org/10.1146/annurev-marine-010213-135046.

Karl, D. M., Beversdorf, L., Björkman, K. M., Church, M. J., Martinez, A., & DeLong, E. F. (2008). Aerobic production of methane in the sea. *Nature Geoscience*, *1*(7), 473–478. https://doi.org/10.1038/ngeo234.

Kaya, K., Morrison, L. F., Codd, G. A., Metcalf, J. S., Sano, T., Takagi, H., et al. (2006). A novel biosurfactant, 2-acyloxyethylphosphonate, isolated from waterblooms of *Aphanizomenon flos-aquae*. *Molecules*, *11*(7), 539–548.

Kennedy, K. E., & Thompson, G. A. (1970). Phosphonolipids: Localization in surface membranes of Tetrahymena. *Science (New York, N.Y.)*, *168*(3934), 989–991. https://doi.org/10.1126/science.168.3934.989.

Kuzuyama, T., Seki, T., Kobayashi, S., Hidaka, T., & Seto, H. (1999). Cloning and expression in *Escherichia coli* of 2-hydroxypropylphosphonic acid epoxidase from the fosfomycin-producing organism, *Pseudomonas syringae* PB-5123. *Bioscience, Biotechnology, and Biochemistry*, *63*(12), 2222–2224. https://doi.org/10.1271/bbb.63.2222.

Liu, P., Liu, A., Yan, F., Wolfe, M. D., Lipscomb, J. D., & Liu, H.-W. (2003). Biochemical and spectroscopic studies on (*S*)-2-hydroxypropylphosphonic acid epoxidase: A novel mononuclear non-heme iron enzyme. *Biochemistry*, *42*(40), 11577–11586. https://doi.org/10.1021/bi030140w.

Liu, P., Murakami, K., Seki, T., He, X., Yeung, S.-M., Kuzuyama, T., et al. (2001). Protein purification and function assignment of the epoxidase catalyzing the formation of fosfomycin. *Journal of the American Chemical Society*, *123*(19), 4619–4620. https://doi.org/10.1021/ja004153y.

Martinez, A., Osburne, M. S., Sharma, A. K., DeLong, E. F., & Chisholm, S. W. (2012). Phosphite utilization by the marine picocyanobacterium *Prochlorococcus* MIT9301. *Environmental Microbiology*, *14*(6), 1363–1377. https://doi.org/10.1111/j.1462-2920.2011.02612.x.

Martinez, A., Tyson, G. W., & DeLong, E. F. (2010). Widespread known and novel phosphonate utilization pathways in marine bacteria revealed by functional screening and metagenomic analyses. *Environmental Microbiology*, *12*(1), 222–238. https://doi.org/10.1111/j.1462-2920.2009.02062.x.

Martinez, A., Ventouras, L. A., Wilson, S. T., Karl, D. M., & DeLong, E. F. (2013). Metatranscriptomic and functional metagenomic analysis of methylphosphonate utilization by marine bacteria. *Frontiers in Microbiology*, *4*, 1–18. https://doi.org/10.3389/fmicb.2013.00340.

McGrath, J. W., Chin, J. P., & Quinn, J. P. (2013). Organophosphonates revealed: New insights into the microbial metabolism of ancient molecules. *Nature Reviews Microbiology*, *11*(6), 412–419. https://doi.org/10.1038/nrmicro3011.

Metcalf, W. W., Griffin, B. M., Cicchillo, R. M., Gao, J., Janga, S. C., Cooke, H. A., et al. (2012). Synthesis of methylphosphonic acid by marine microbes: A source for methane in the aerobic ocean. *Science (New York, N.Y.)*, *337*(6098), 1104–1107. https://doi.org/10.1126/science.1219875.

Metcalf, W. W., & Wanner, B. L. (1991). Involvement of the *Escherichia coli phn* (*psiD*) gene cluster in assimilation of phosphorus in the form of phosphonates, phosphite, Pi esters, and Pi. *Journal of Bacteriology*, *173*(2), 587–600.

Metcalf, W. W., & Wanner, B. L. (1993a). Evidence for a fourteen-gene, *phnC* to *phnP* locus for phosphonate metabolism in *Escherichia coli*. *Gene*, *129*(1), 27–32. https://doi.org/10.1016/0378-1119(93)90692-V.

Metcalf, W. W., & Wanner, B. L. (1993b). Mutational analysis of an *Escherichia coli* fourteen-gene operon for phosphonate degradation, using TnphoA' elements. *Journal of Bacteriology*, *175*(11), 3430–3442.

Nair, S. K., & van der Donk, W. A. (2011). Structure and mechanism of enzymes involved in biosynthesis and breakdown of the phosphonates fosfomycin, dehydrophos, and phosphinothricin. *Archives of Biochemistry and Biophysics*, *505*(1), 13–21. https://doi.org/10.1016/j.abb.2010.09.012.

Parker, G. F., Higgins, T. P., Hawkes, T., & Robson, R. L. (1999). *Rhizobium (Sinorhizobium) meliloti phn* genes: Characterization and identification of their protein products. *Journal of Bacteriology*, *181*(2), 389–395.

Peck, S. C., Chekan, J. R., Ulrich, E. C., Nair, S. K., & van der Donk, W. A. (2015). A common late-stage intermediate in catalysis by 2-hydroxyethyl-phosphonate dioxygenase and methylphosphonate synthase. *Journal of the American Chemical Society*, *137*(9), 3217–3220. https://doi.org/10.1021/jacs.5b00282.

Peck, S. C., Cooke, H. A., Cicchillo, R. M., Malova, P., Hammerschmidt, F., Nair, S. K., et al. (2011). Mechanism and substrate recognition of 2-hydroxyethylphosphonate dioxygenase. *Biochemistry*, *50*(30), 6598–6605. https://doi.org/10.1021/bi200804r.

Peck, S. C., & van der Donk, W. A. (2017). Go it alone: Four-electron oxidations by mononuclear non-heme iron enzymes. *Journal of Biological Inorganic Chemistry*, *22*(2–3), 381–394. https://doi.org/10.1007/s00775-016-1399-y.

Peck, S. C., Wang, C., Dassama, L. M. K., Zhang, B., Guo, Y., Rajakovich, L. J., et al. (2017). O-H activation by an unexpected ferryl intermediate during catalysis by 2-hydroxyethylphosphonate dioxygenase. *Journal of the American Chemical Society*, *139*(5), 2045–2052. https://doi.org/10.1021/jacs.6b12147.

Podzelinska, K., He, S., Soares, A., Zechel, D. L., Hove-Jensen, B., & Jia, Z. (2008). Expression, purification and preliminary diffraction studies of PhnP. *Acta Crystallographica. Section F, Structural Biology and Crystallization Communications*, *64*(Pt 6), 554–557. https://doi.org/10.1107/S1744309108014656.

Podzelinska, K., He, S. M., Wathier, M., Yakunin, A., Proudfoot, M., Hove-Jensen, B., et al. (2009). Structure of PhnP, a phosphodiesterase of the carbon-phosphorus lyase pathway for phosphonate degradation. *The Journal of Biological Chemistry*, *284*(25), 17216–17226. https://doi.org/10.1074/jbc.M808392200.

Polyviou, D., Hitchcock, A., Baylay, A. J., Moore, C. M., & Bibby, T. S. (2015). Phosphite utilization by the globally important marine diazotroph Trichodesmium. *Environmental Microbiology Reports*, 7(6), 824–830. https://doi.org/10.1111/1758-2229.12308.

Randerath, K., & Randerath, E. (1966). Ion-exchange thin-layer chromatography. XV. Preparation, properties and applications of paper-like PEI-cellulose sheets. *Journal of Chromatography*, *22*(1), 110–117.

Reeburgh, W. S. (2007). Oceanic methane biogeochemistry. *Chemical Reviews*, *107*(2), 486–513. https://doi.org/10.1021/cr050362v.

Ren, Z., Ranganathan, S., Zinnel, N. F., Russell, W. K., Russell, D. H., & Raushel, F. M. (2015). Subunit interactions within the carbon-phosphorus lyase complex from *Escherichia coli*. *Biochemistry*, *54*(21), 3400–3411. https://doi.org/10.1021/acs.biochem.5b00194.

Repeta, D. J., Ferrón, S., Sosa, O. A., Johnson, C. G., Repeta, L. D., Acker, M., et al. (2016). Marine methane paradox explained by bacterial degradation of dissolved organic matter. *Nature Geoscience*, *9*(12), 884–887. https://doi.org/10.1038/ngeo2837.

Scranton, M. I., & Brewer, P. G. (1977). Occurrence of methane in the near-surface waters of the western subtropical North-Atlantic. *Deep Sea Research*, *24*(2), 127–138. https://doi.org/10.1016/0146-6291(77)90548-3.

Seibert, C. M., & Raushel, F. M. (2005). Structural and catalytic diversity within the amidohydrolase superfamily. *Biochemistry*, *44*(17), 6383–6391. https://doi.org/10.1021/bi047326v.

Seidel, H. M., Freeman, S., Seto, H., & Knowles, J. R. (1988). Phosphonate biosynthesis: Isolation of the enzyme responsible for the formation of a carbon-phosphorus bond. *Nature*, *335*(6189), 457–458. https://doi.org/10.1038/335457a0.

Seweryn, P., Van, L. B., Kjeldgaard, M., Russo, C. J., Passmore, L. A., Hove-Jensen, B., et al. (2015). Structural insights into the bacterial carbon-phosphorus lyase machinery. *Nature*, *525*(7567), 68–72. https://doi.org/10.1038/nature14683.

Shames, S. L., Wackett, L. P., LaBarge, M. S., Kuczkowski, R. L., & Walsh, C. T. (1987). Fragmentative and stereochemical isomerization probes for homolytic carbon to phosphorus bond scission catalyzed by bacterial carbon-phosphorus lyase. *Bioorganic Chemistry*, *15*(4), 366–373. https://doi.org/10.1016/0045-2068(87)90033-2.

Shao, Z., Blodgett, J. A. V., Circello, B. T., Eliot, A. C., Woodyer, R., Li, G., et al. (2008). Biosynthesis of 2-hydroxyethylphosphonate, an unexpected intermediate common to multiple phosphonate biosynthetic pathways. *The Journal of Biological Chemistry*, *283*(34), 23161–23168. https://doi.org/10.1074/jbc.M801788200.

Shisler, K. A., & Broderick, J. B. (2012). Emerging themes in radical SAM chemistry. *Current Opinion in Structural Biology*, *22*(6), 701–710. https://doi.org/10.1016/j.sbi.2012.10.005.

Sosa, O. A., Repeta, D. J., Ferrón, S., Bryant, J. A., Mende, D. R., Karl, D. M., et al. (2017). Isolation and characterization of bacteria that degrade phosphonates in marine dissolved organic matter. *Frontiers in Microbiology*, *8*, 1786. https://doi.org/10.3389/fmicb.2017.01786.

Van Mooy, B. A. S., Fredricks, H. F., Pedler, B. E., Dyhrman, S. T., Karl, D. M., Koblížek, M., et al. (2009). Phytoplankton in the ocean use non-phosphorus lipids in response to phosphorus scarcity. *Nature*, *458*(7234), 69–72. https://doi.org/10.1038/nature07659.

Villarreal-Chiu, J., & Quinn, J. (2012). The genes and enzymes of phosphonate metabolism by bacteria, and their distribution in the marine environment. *Frontiers in Microbiology*, *3*, 1–13. https://doi.org/10.3389/fmicb.2012.00019.

Wackett, L. P., Shames, S. L., Venditti, C. P., & Walsh, C. T. (1987). Bacterial carbon-phosphorus lyase: Products, rates, and regulation of phosphonic and phosphinic acid metabolism. *Journal of Bacteriology*, *169*(2), 710–717.

Wackett, L. P., Wanner, B. L., Venditti, C. P., & Walsh, C. T. (1987). Involvement of the phosphate regulon and the *psiD* locus in carbon-phosphorus lyase activity of *Escherichia coli* K-12. *Journal of Bacteriology*, *169*(4), 1753–1756.

Wang, C., Chang, W.-C., Guo, Y., Huang, H., Peck, S. C., Pandelia, M. E., et al. (2013). Evidence that the fosfomycin-producing epoxidase, HppE, is a non-heme-iron peroxidase. *Science (New York, N.Y.)*, *342*(6161), 991–995. https://doi.org/10.1126/science.1240373.

Wang, J., Woldring, R. P., Román-Meléndez, G. D., McClain, A. M., Alzua, B. R., & Marsh, E. N. G. (2014). Recent advances in radical SAM enzymology: New structures and mechanisms. *ACS Chemical Biology*, *9*(9), 1929–1938. https://doi.org/10.1021/cb5004674.

Wanner, B. L. (1993). Gene regulation by phosphate in enteric bacteria. *Journal of Cellular Biochemistry*, *51*(1), 47–54. https://doi.org/10.1002/jcb.240510110.

Watanabe, Y., Nakajima, M., Hoshino, T., Jayasimhulu, K., Brooks, E. E., & Kaneshiro, E. S. (2001). A novel sphingophosphonolipid head group 1-hydroxy-2-aminoethyl phosphonate in *Bdellovibrio stolpii*. *Lipids*, *36*(5), 513–519. https://doi.org/10.1007/s11745-001-0751-3.

Whitteck, J. T., Malova, P., Peck, S. C., Cicchillo, R. M., Hammerschmidt, F., & van der Donk, W. A. (2011). On the stereochemistry of 2-hydroxyethylphosphonate dioxygenase. *Journal of the American Chemical Society*, *133*(12), 4236–4239. https://doi.org/10.1021/ja1113326.

Woschek, A., Wuggenig, F., Peti, W., & Hammerschmidt, F. (2002). On the transformation of (*S*)-2-hydroxypropylphosphonic acid into fosfomycin in *Streptomyces fradiae*—A unique method of epoxide ring formation. *ChemBioChem*, *3*(9), 829–835. https://doi.org/10.1002/1439-7633(20020902)3:9<829::AID-CBIC829>3.0.CO;2-V.

Yan, F., Munos, J. W., Liu, P., & Liu, H.-W. (2006). Biosynthesis of Fosfomycin, re-examination and re-confirmation of a unique Fe(II)- and NAD(P)H-dependent epoxidation reaction. *Biochemistry*, *45*(38), 11473–11481. https://doi.org/10.1021/bi060839c.

Yang, K., Ren, Z., Raushel, F. M., & Zhang, J. (2016). Structures of the carbon-phosphorus lyase complex reveal the binding mode of the NBD-like PhnK. *Structure*, *24*(1), 37–42. https://doi.org/10.1016/j.str.2015.11.009.

Yu, X., Doroghazi, J. R., Janga, S. C., Zhang, J. K., Circello, B., Griffin, B. M., et al. (2013). Diversity and abundance of phosphonate biosynthetic genes in nature. *Proceedings of the National Academy of Sciences of the United States of America*, *110*(51), 20759–20764. https://doi.org/10.1073/pnas.1315107110.

Yu, X., Price, N. P. J., Evans, B. S., & Metcalf, W. W. (2014). Purification and characterization of phosphonoglycans from *Glycomyces* sp. strain NRRL B-16210 and *Stackebrandtia nassauensis* NRRL B-16338. *Journal of Bacteriology*, *196*(9), 1768–1779. https://doi.org/10.1128/JB.00036-14.

Zhu, H., Peck, S. C., Bonnot, F., van der Donk, W. A., & Klinman, J. P. (2015). Oxygen-18 kinetic isotope effects of nonheme iron enzymes HEPD and MPnS support iron(III) superoxide as the hydrogen abstraction species. *Journal of the American Chemical Society*, *137*(33), 10448–10451. https://doi.org/10.1021/jacs.5b03907.